WILEY-VCH

DOI: 10.1002/ ((please add manuscript number))
**Article type: Progress Report**

# Functionalization of 2D materials with photosensitive molecules: from light-responsive hybrid systems to multifunctional devices

*Yuda Zhao, Stefano Ippolito, and Paolo Samorì**

Dr. Y. Zhao, S. Ippolito, Prof. P. Samorì
University of Strasbourg, CNRS, ISIS UMR 7006, 8 allée Gaspard Monge, F-67000 Strasbourg, France
E-mail: samorì@unistra.fr

Keywords: 2D material, photochromic molecules, light responsive, device, functionalization

**Abstract**

Two-dimensional materials possess exceptional physical and chemical properties which render them appealing components for numerous potential applications in (opto)electronics, energy storage, sensing and biomedicine. However, such unique properties are hardly tunable or modifiable. The functionalization of 2D crystals with molecules constitutes a powerful strategy to adjust and modulate their properties, by also imparting them new functions. In this framework, the combination of 2D materials with photo-sensitive molecules is a viable route for harnessing their light-responsive nature. The latter takes full advantage of the extremely high sensitivity of 2D materials to subtle changes in the local environment and the capacity of photosensitive molecules to modify their intrinsic properties when exposed to electromagnetic fields. The hybrid molecule-2D materials can preserve the unique optical and electrical properties of 2D layers and can exhibit additional light-tunable features. In this Progress Report, the protocols which can be pursued for the 2D materials functionalization and switching mechanisms in photosensitive systems are reviewed, followed by an in-depth discussion on their tunable optical properties and their exploitation when integrated in novel photoswitchable electronic devices. The opportunities and associated challenges to be tackled for the development of unprecedented and high-performance light-responsive devices are discussed.

## 1. Introduction

Two-dimensional (2D) materials display outstanding optical, electrical, mechanical and thermal characteristics which result from their atomic thickness.[1, 2] Such unique properties endorsed them as ideal building blocks for exploring novel physical phenomena. Remarkably, graphene and other 2D materials, including elemental 2D systems (phosphorene, silicene etc.) and transition metal dichalcogenides (TMDs, such as $MoS_2$, $WSe_2$, etc.), show dramatically different optical and electrical properties when compared with their bulk counterparts.[3-5] Such a feature inspired scientists to explore possible applications of 2D materials in flexible and nanoscale (opto)electronics.[6-9]

Graphene, the ancestor of 2D material's family, is a semimetal with a zero bandgap. Because of its large conductivity, high carrier mobility, and large surface area, graphene was elected as ideal material to construct flexible electrodes for opto-electronics and energy applications.[10] Monolayer and few-layer TMDs, with a sizable bandgap and high charge carrier mobilities, are promising semiconducting materials for field-effect transistors (FETs) and diodes.[11-13] Because of their highest surface-to-volume ratio, the properties 2D materials are extremely sensitive to the environmental changes, making them ideal active components for sensing applications.[14]

The practical application of 2D materials in tomorrow's opto-electronics require the fine modulation of various physical properties, and especially the carrier type and concentration. In contrast to the conventional doping methods employed for inorganic semiconductors, the doping of 2D materials can take place either *via* charge transfer or *via* dipolar interactions. To explore both effects, molecules with electron-donating or electron-accepting groups as well as molecules exposing a polar head-group have been successfully adsorbed as dopants on the surface of the 2D materials to tune their carrier density.[15-17] More generally, the bottom-up tailoring of the interactions between molecule and 2D materials also represents a smart way to widen the functionality of the latter components. This result can be accomplished by taking

advantage of the almost unlimited degrees of freedom offered by chemistry on the design and synthesize molecules integrating specific functional groups. One interesting characteristic that can be programmed in molecules and assemblies thereof is their ability to respond to external stimuli (light-irradiation, changes in pH, electrochemical stimuli, magnetic fields, etc.) by changing their state. Importantly, each state exhibits well-defined physical and chemical properties which can in turn be used to modulate the properties of adjacent 2D materials.

As an infinite source of inspiration, nature displays abundant examples of stimuli-responsive systems, such as the rapid movement of the leaves of Mimosa pudica when touched and the skin color change of chameleons according to the outer environment. Motivated by these dynamic living systems, artificial stimuli-responsive systems have been developed to mimic these unique properties and realize smart functionalities for future electronic and biomedical applications.[18, 19] Among various external stimuli, light displays several advantages as it features a high spatio-temporal control, it is non-invasive since it can operate in non-contact for remote applications, it can be modulated *via* the fine tuning of the power and dose, and it leaves no side products.[20-22]

Among light-sensitive molecules, photochromes are small organic molecules which are able to undergo efficient and reversible photochemical isomerization between (at least) two (meta)stable states exhibiting markedly different properties. The light-triggered modification of the properties at the single molecular level are translated into changes in the characteristics of the materials thereof,[23] making this class of materials extremely useful for a variety of applications such as information storage, actuators and energy storage.[24-26] Within this context, the functionalization of 2D materials with photochromic molecules can offer a special opportunity for modulating their properties as a result of light stimuli, to ultimately develop novel 2D light-responsive devices. The hybrid light-responsive system can be expected not only to virtually preserve the unique characteristics of 2D crystals and photochromic molecules, but also to offer the emergence of novel properties and applications.

Alongside photochromic molecules, some other photosensitive molecules possessing high optical absorption or responsivity have also been exploited in order to optimize the performance of 2D light-responsive devices.[27, 28]

In this Progress Report, we review the most enlightening results reported on the optically-responsive hybrid system composed of 2D materials and photosensitive molecules. We provide guidelines for the controlled functionalization of 2D materials using covalent and non-covalent approaches. We discuss the strategies to harness the dynamic change of the properties of the 2D materials, and we highlight the most relevant applications of such hybrid systems in (opto)electronic and energy devices. Finally, we provide perspectives on the future development of such hybrid systems to underscore their brightest future.

## 2. Functionalization of 2D layers with molecular systems

The extraordinary properties singled out on graphene, resulting from its exotic physics and phenomena confined to the atomically thin limit, has triggered a tremendous effort focused on the isolation and production of other 2D materials beyond graphene. Importantly, the exfoliation of various hundreds of layered materials, holding unique properties, became possible. Besides their inherent properties, during the last few years the scientific community has focused the attention on molecular approaches aimed at finely tuning the properties of 2D materials, by exploiting the enormous library of molecular systems. Indeed, the fabrication of novel 2D material-based devices bearing unusual functionalities is considered an attractive area in current material science-oriented research. 2D materials can be functionalized with light-responsive,[29] magneto-responsive[30] and electrochemically-switchable moieties,[31] to take advantage of the properties of the different building blocks in order to obtain superior hybrid devices *via* synergic effects of the components, with the ultimate goal of fabricating hybrid and multifunctional devices which exhibit new and/or enhanced properties and performances. It is worth mentioning that the functionalization strategies can take place by

means of both solution-based and vapor-based approaches, although the former represents the overwhelming majority of works reported in literature because of a major versatility. In light of the previous considerations, the combination of 2D materials with photo-responsive molecular systems represents a prime tempting and challenging perspective, with the long-term target being the emergence of disruptive technologies for multifunctional (opto)electronic applications. In this framework, several different light-sensitive molecular systems have been employed, spanning from simple molecules to complex structures obtained by means of multi-step synthetic approaches (**Figure 1**).

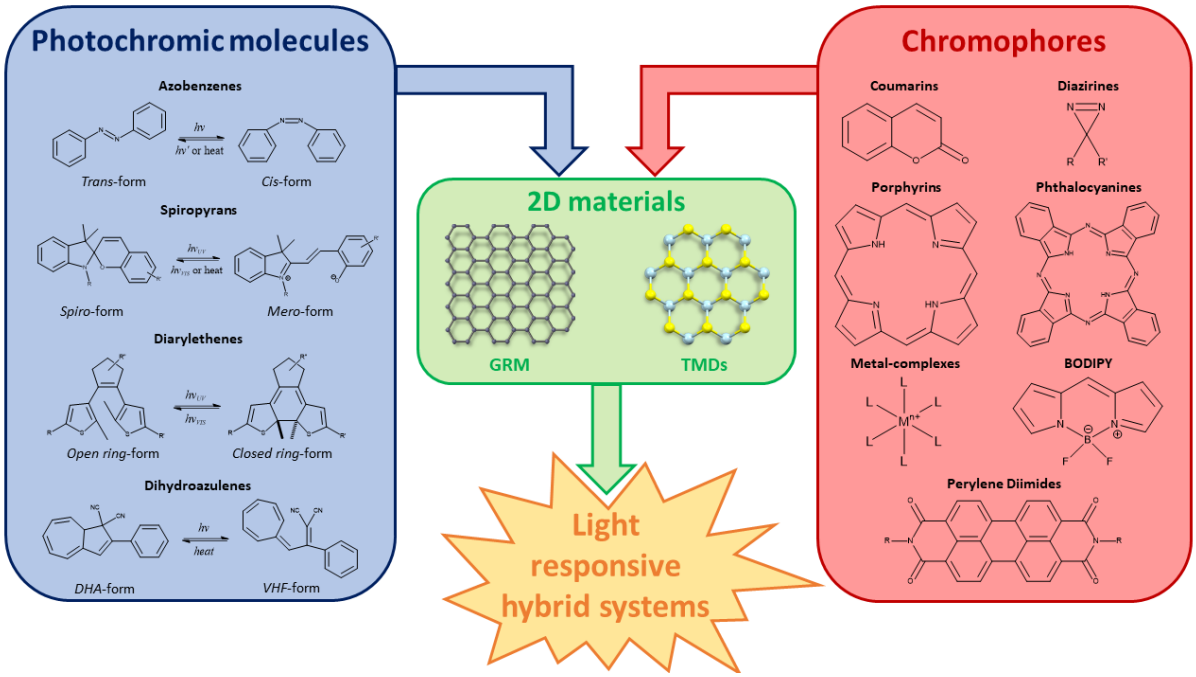


**Figure 1.** Illustration of the most common photoresponsive molecular systems employed to functionalize 2D structures, such as graphene-related materials (GRM) and transition metal dichalcogenides (TMDs), and attain light-responsive hybrid systems. For the sake of righteousness, the distinction between photochromic molecules and chromophores is underlined.

### 2.1. Light-responsive molecules: a brief overview

As results of their intrinsic photochemical and photophysical properties, molecules can respond to light stimuli in two ways. Upon absorption of photons with well-defined energy, molecules can either be reversibly toggled between two or more states (*via* photoisomerization) or they can get temporary promoted to excited states. More specifically,

the first aforementioned family refers to photochromic molecules, which could be exploited to reversibly tune the properties of functionalized hybrid 2D systems. The most popular representatives of such a class of molecules are azobenzenes, spiropyrans, diarylethenes and dihydroazulenes.

The photochromic properties of azobenzenes were investigated for the first time in 1937 by Hartley and co-workers, who studied the influence of light absorption on the configuration of N=N double bond, also known as azo group.[32] Likewise the C=C double bond, the N=N double bond in azobenzenes have two geometric isomers (*cis* or Z and *trans* or E) with the *trans* form being ~ 12 Kcal $mol^{-1}$ more stable than the *cis* isomer.[33] The energy barrier for the photoisomerization process E → Z is ~ 23 Kcal $mol^{-1}$, therefore the *trans* isomer is thermodynamically stable and predominant in the dark and room temperature conditions.[34] The *trans* azobenzene can undergo isomerization to *cis* form upon irradiation with a wavelength between 320-350 nm (on the picosecond timescale) and the reverse reaction takes place when *cis* isomers are irradiated with a wavelength between 400-450 nm (in a slower timescale, from milliseconds to days).[35] Because of the metastable nature of the *cis* form, the back isomerization to the *trans* isomer can also take place thermally (e.g. at room temperature). The (photo)isomerization process induces remarkable changes in the physical and chemical properties of the molecule, such as in the absorption spectrum, molecular geometry and dipole moment.[36]

Firstly explored and studied during the first half of the twentieth century, spiropyrans are photochromic molecules characterized by a pericyclic reaction.[37] The neutral spiropyran molecule undergoes a reversible photochemical cleavage of the C-O bond in the closed-ring form yielding a zwitterionic open-ring form called merocyanine. The back-isomerization can be triggered either thermally photochemically. In both cases the rate-determining step is the C-O cleavage in the pyran ring, which is followed by a stabilization process driven by the Z-E isomerization around the spiro- and pyran-bridging double bond. Therefore, merocyanine may

exist in different Z/E isomers but, due to the low thermal stability of the isomer with the central Z double bond, only the form showing the central E double bond is observed at room temperature. Such a thermodynamically stable isomer is known as *trans-trans-cis* (TTC) form.[38] The ring-opening reaction, induced by photochemical stimuli, occurs upon UV irradiation of the spiropyran isomer (UV light, $\lambda \sim 365$ nm) and leads to the metastable zwitterionic merocyanine isomer.[39] In particular, by considering the inherent different photophysical and photochemical properties of the structures involved in the switching mechanisms, spiropyrans might be employed to build multi-state molecular switches, sensitive to both physical and chemical stimuli, such as light and pH respectively.[40, 41] Ultimately, the reversible photoinduced spiropyran → merocyanine reaction entails large variations in the physicochemical properties of the system, such as in the dipole moment and molecular geometry,[38, 39, 42, 43] making spiropyrans prime components to generate radiative stimuli-responsive hybrid materials.

Diarylethenes, being another member of the photochromic molecules family, have been pioneered by Irie and co-workers in the late 1980s.[44] They possess a peculiar characteristic: both the open and closed isomers, which are accessible with light-stimuli, are thermodynamically stable due to the large activation energy of the reaction mechanisms involved in the isomerization process.[45] In particular, diarylethenes are characterized by a reversible photochemical 6π-electrocyclization and 6π-cycloreversion reaction occurring between the open-ring 1,3,5-hexatriene and the closed-ring 1,3-hexadiene isomer. A paramount difference between the two isomers concerns their conjugation: in the open-ring structure, the conjugation is localized on the heteroaromatic rings, whereas the closed-form π-conjugation delocalizes electrons over the whole backbone of the molecule, resulting in a lower gap between the highest occupied molecular orbital (HOMO) and the lowest unoccupied molecular orbital (LUMO) compared to its open counterpart.[46] The photoisomerization between the open and the closed form is reversible. While UV light

exposure enables open → close isomerization, the back process is triggered by visible light. The isomerization process is accompanied by drastic changes in the physicochemical properties of the molecules, which can be exploited as photosensitive systems for electronics and data storage.[47]

The last example of photochromic system is represented by the dihydroazulenes (DHA), whose photochemical properties were investigated for the first time in the early 1980s by Daub *et al*.[48] The photochromism of dihydroazulenes is based on two different types of electrocyclic reactions: a photochemically induced ring-opening reaction of azulene derivatives to the metastable vinylheptafulvalene isomer, followed by thermally assisted ring-closure reaction of vinylheptafulvalene to dihydroazulenes. The aforementioned 10π-electron rearrangement occurs when dihydroazulenes molecules are irradiated with UV light (λ ~ 365 nm), leading to the non-fluorescent vinylheptafulvalene species, whose thermal-induced back-reaction exhibits an activation energy of 18-21 Kcal $mol^{-1}$.[49, 50] Experimental studies, performed about the dynamics of the photochemical ring-opening reaction, showed that both decay of transient absorption of $S_1$-excited dihydroazulenes and rise of the stationary $S_0$-$S_1$ absorption of the photoproduct occur monoexponentially, with a lifetime ($\tau_{DHA}$) of about 600 fs. Furthermore, the photochemical properties of vinylheptafulvalene (lack of fluorescence at any temperature and hindered photoinduced ring-closure reaction) can be explained by a very short $S_1$ state lifetime and significant potential barrier between the $S_1$ states of the vinylheptafulvalene and dihydroazulene isomers.[50] Ultimately, the dihydroazulenes/vinylheptafulvalene pair could represent an ideal and versatile model to exploit in the fabrication of multi-stimuli-responsive hybrid 2D materials, with particular emphasis on the optoelectronic applications.

The photochemical properties of the above-mentioned photochromic molecules are summarized in **Table 1**. The general properties described above for the various types of photochromic molecules are those associated to their non-functionalized derivatives, hence

their functionalization could represent an additional powerful tool to finely tailor their properties, which will be discussed in section 2.2 and 2.3 below.

**Table 1**. Photochemical properties of the photochromic molecules

| Photochromic molecules | Reactions | Wavelength | Ref. |
|---|---|---|---|
| Azobenzenes | E → Z Photoisomerization | UV (320 nm < λ < 350 nm) | [35] |
| | Z → E Photoisomerization | Vis (400 nm < λ <450 nm) or Δ | |
| Spiropyrans | Electrocyclic ring-opening | UV (λ ~ 365 nm) | [38] |
| | Electrocyclic ring-closing | Vis (λ ~ 635 nm) or Δ | |
| Diarylethenes | 6π-electrocyclization | UV (λ ~ 365 nm) | [44] |
| | 6π-cycloreversion | Vis (λ ~ 635 nm) | |
| Dihydroazulenes | Electrocyclic ring-opening | UV (λ ~ 365 nm) | [49] |
| | Electrocyclic ring-closing (thermally-assisted) | Δ (~ 60 °C) | |

Note: Δ = Heat. The reported approximate wavelength values and ranges can be affected by molecular structural changes.

The second group of photosensitive systems comprises molecules possessing, in most cases, a HOMO-LUMO energy difference within the visible range of the electromagnetic spectrum. Such molecules are called chromophores. When photons with a well-distinct energy hit the chromophore molecules, they can be absorbed by exciting an electron from its ground state into an excited state. Hence, the return process to the initial ground state can occur *via* either thermal or radiative relaxation (or a combination of the two). For radiative relaxations, light with a specific wavelength is emitted. The most representative members of such a family are coumarins, porphyrins, phthalocyanines, metal complexes, BODIPY, perylene diimides and diazirines derivatives. It is also worth mentioning the family of viologens, which are molecular systems possessing very interesting and versatile photochemical properties, able to switch among different oxidation states, each one characterized by specific light-sensitivity.[51] Nevertheless, viologens are electrochemical switching systems and even if they represent a fascinating class of photosensitive molecules, they go beyond the scope of this Progress Report.

Coumarins are aromatic natural compounds which can be found numerous plants and leaves of various cherry blossom trees. They were synthesized for the first time in the second half of the nineteenth century by Perkin,[52] but the photochemical properties were investigated almost one century later by Mattoo.[53] Unsubstituted coumarins are not fluorescent and for

such a reason coumarin derivatives have been designed to boost photosensitivity; in particular, inductive and mesomeric effects of the substituents in the 7-substituted coumarin derivative yields an increase in the fluorescence.[54] Nowadays, coumarin derivatives are quite versatile structures and the nature of substituents in the molecular architecture plays a fundamental role to prepare dyes whose emission covers the whole visible spectrum.[55]

Porphyrins are an important class of natural photosensitive compounds playing a fundamental role in the metabolism of living organisms. The unsubstituted structure, called porphine, is composed of four pyrrole rings linked by four methine bridges, with 22 conjugated π-electrons among which only 18 are delocalized according to the Hückel's rule of aromaticity (4n+2 delocalized π-electrons, where n = 4). Although the first synthesis by Rothemund dates back to the 1935,[56] the spectroscopic properties of porphyrins were investigated during the second half of the twentieth century, considering the effects of substituents on the photochemical properties.[57, 58] The latter are mainly characterized by $\pi \rightarrow \pi^*$ electronic transitions, and a typical porphyrin absorption spectrum features two distinct regions. The first one involves the transition from the ground state to the second excited state ($S_0 \rightarrow S_2$), known as Soret or B band, and ranges from 350 nm to 450 nm. The second region describes a weaker transition from the ground state to the first excited state ($S_0 \rightarrow S_1$), known as Q band, and range from 450 nm to 700 nm.[59] Conversely, in an emission spectrum of porphyrins, due to a highly efficient $S_2 \rightarrow S_1$ internal conversion mechanism, fluorescence is detected only for the Q band, related to the $S_1 \rightarrow S_0$ transition.[60] Ultimately, peripheral substituents on the porphyrin ring, along with the possible protonation of two of the inner nitrogen atoms or the insertion/change of metal atoms into the macrocycle, strongly affect the photochemical properties of the system,[60] with possible interesting applications in optoelectronics.

Phthalocyanines are large macrocycles and two-dimensional 18 π-electron aromatic synthetic analogues of porphyrins. The phthalocyanine molecule consists of four isoindole units linked by nitrogen atoms and the first study about structural and physicochemical properties dates

back to the early 1930s, performed by Sir Linstead.[61] The photochemistry of phthalocyanines is similar to that of porphyrins, being characterized by a strong and generally well-resolved absorption band, known as Q band, which lies in the range between 650 to 670 nm.[62] Likewise porphyrin, the incorporation of metal ions inside the central cavity and the presence of substituents strongly affects the response to light-stimuli,[63] making phthalocyanine a versatile and powerful tool to employ in the fabrication of photosensitive hybrid systems for (opto)electronic and biomedicine applications (Q band lies at the beginning of the first optical window for biological tissues).[64-66]

An additional class of well-known chromophores is represented by metal complexes, namely coordination complexes in which a metal atom or ion (coordination center) is surrounded by an array of bound molecular systems (ligands or complexing agents). In the last few decades, photosensitive metal complexes have attracted a great attention due to their promising and versatile physico-chemical properties which make them appealing for several applications, such as optoelectronics,[67] bioimaging,[68] and biosensing[69]. The photochemical properties are strictly related to the nature of the metallic center and anchoring ligands, whose electronic transitions to the excited states and inherent photoredox mechanisms influence the resulting photoluminescence (PL).[70] In particular, the excited states generated upon photon absorption are obtained *via* electron transfer either from the full ligand molecular orbitals to the partially filled metal *d*-orbitals or from the partially full metal *d*-orbitals to the low-energy empty ligand orbitals, ligand-to-metal charge transfer (LMCT) and metal-to-ligand charge transfer (MLCT) respectively. Therefore, the use of different metallic centers (typically transition metals or lanthanides) and ligands guarantees the production of versatile chromophores, whose PL can range in the whole visible spectrum.[67]

BODIPY are molecules possessing intriguing properties for the fabrication of novel hybrid 2D material-based devices. The acronym stands for boron-dipyrromethenes, a family of fluorescent dyes made of organoboron compounds in which dipyrromethene is complexed by

a disubstituted boron center, usually $BF_2$. Unsubstituted BODIPY molecules are photosensitizers characterized by favorable extinction coefficient and light to dark toxicity, whilst the core structure possesses a considerable limitation related to the high hydrophobicity. Such a restriction can be overcame by properly modifying the structure of the molecules,[71] mainly designed to maximize biological compatibility and activity for bioimaging applications[72] and photodynamic cancer therapy.[73]

Perylene-3,4,9,10-tetracarboxylic acid diimide derivates, commonly called perylene diimides, represent an additional intriguing class of photosensitive molecular systems, firstly reported in the early 1910s and mainly used as industrial pigments until the late 1950s.[74] They exhibit an extreme versatility in terms of chemical and physical properties, achieved by proper designing of the substituents especially in the imide *N,N'* positions and in the 1,6,7 and 12 positions of the hydrocarbon core, also called bay positions.[75] In particular, the imide substituents have minimal effects on the optical and electronic properties but can be used to affect solubility and aggregation phenomena, whereas the substituents in bay positions strongly affect the electronic and optical properties of such molecular systems.[76] Indeed, perylene diimides can be described as chromophores with a $S_0$-$S_1$ transition (well described as HOMO-LUMO excitation) polarized along the long molecular (N-N) axis, since the HOMO and LUMO nodal planes are localized at the imide nitrogen atoms.[77] In terms of optical properties, an additional pivotal aspect for such molecular systems is represented by their near-unity fluorescence quantum yields,[78] which guarantee the fabrication of high-performance devices when perylene diimides are involved.[79, 80] Nowadays, taking advantages of the photo, thermal and chemical stability of these light-sensitive molecules, perylene diimides and larger rylenes are widely used in light-harvesting,[81] photocatalysis[82] and optoelectronic applications[83].

The final example of chromophores is diazirines, being among the smallest photoreactive groups and consist of a carbon atom bound to two nitrogen atoms, which are double-bonded

to each other forming a 3-membered ring known as 3H-DA. Upon UV light irradiation (λ ~ 360 nm), diazirines undergo photolysis generating the reactive carbenes, carbon intermediated containing two non-bonding orbitals with two options of divisions for the two electrons between them: singlet and triplet, depending on the nature of substituents. In addition to the small size, diazirines present additional advantages such as thermal stability, short lifetime upon irradiation and consequent high reactivity, justifying the broad range of applications spanning from biological systems to electronics.[84, 85] **Table 2** summarizes the photochemical properties of the aforementioned chromophores.

**Table 2**. Photochemical properties of chromophores

| Chromophores | Absorption range (HOMO → LUMO) | Fluorescence range (LUMO → HOMO) | Ref. |
|---|---|---|---|
| Coumarins | 250 nm < λ < 600 nm | Whole visible spectrum | [53] |
| Porphyrins | 350 nm < λ < 450 nm (Soret)<br>450 nm < λ < 700 nm (Q band) | 600 nm < λ < 750 nm | [58] |
| Phthalocyanines | 650 nm < λ < 670 nm (Q band) | 660 nm < λ < 800 nm | [61] |
| Metal-complexes | Whole visible spectrum | Whole visible spectrum | [66] |
| BODIPY | Whole visible spectrum | Whole visible spectrum | [70] |
| Perylene Diimides | 400 nm < λ < 600 nm | 500 nm < λ < 750 nm | [75] |
| Diazirines | UV (λ ~ 360 nm) | ---- | [83] |

Note: Whole visible spectrum = Photochemical properties can be tuned by proper designing of the substituents.

At the end of this brief journey through the most captivating and promising light-responsive molecular systems, hereafter we focus on the approaches to combine them with 2D materials. In this regard, the functionalization strategies to couple photosensitive molecules to 2D crystals mainly rely on either covalent or non-covalent approaches (**Figure 2**). Although both of them can yield drastic changes in the properties of hybrid 2D systems, the two strategies exhibit different effects due to the characteristic features detailed below.

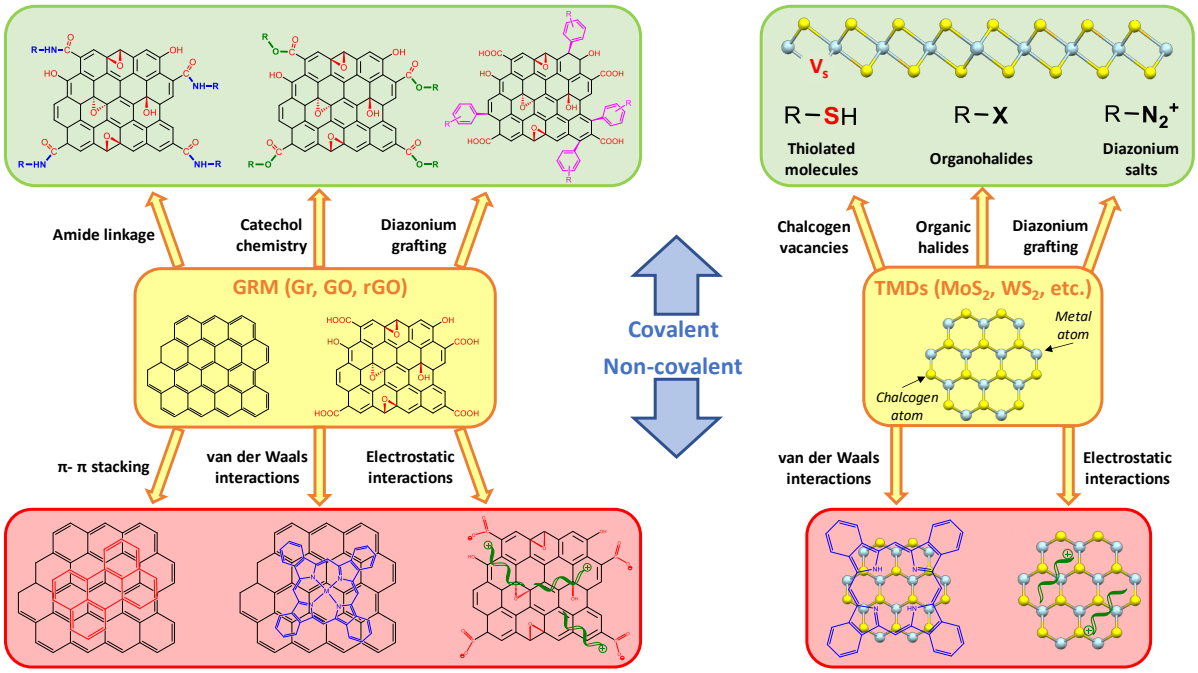


**Figure 2.** The depiction illustrates the main covalent (top) and non-covalent (bottom) strategies adopted to functionalize graphene-related materials, GRM, (left) and transition metal dichalcogenides, TMDs, (right) materials.

### 2.2. Non-covalent functionalization

The all-surface-and-zero-volume character of 2D materials fosters their interaction with surrounding molecular systems. This can take place through non-covalent forces, i.e. *via* molecular physisorption. Such physical interaction, whose energies are within the range of $10^{-1}$ - 10 kcal $mol^{-1}$, does not involve the formation of new chemical bonds, and they include electrostatic, π-π stacking, van der Waals and hydrophobic forces. Non-covalent functionalization is quite popular in the world of 2D systems, both for carbon-based nanomaterials, such as the graphene-related materials (GRM),[86, 87] and materials beyond graphene, such as TMDs.[15] The molecular design comprises an anchoring group featuring a high affinity for the basal plane of the 2D material to guarantees physisorption and a functional moiety for imparting a new function to the monolayer. The latter can encompass molecules presented in section 2.1 above and displayed in Figure 1.

Physical adsorption of molecules holds the unique advantage of leaving the crystal structure of the 2D materials unaltered, maintaining their superior optoelectronic properties. Being

based on weak and reversible non-covalent interactions, exchange of components can be foreseen.[88-90] Although non-covalent anchoring strategies are less robust under the preparation and operating conditions (annealing temperature, vacuum, etc.), they offer superior compatibility towards the functional groups of the reacting species. Among the various non-covalent physical interaction which can be used to immobilize molecules on the surfaces of 2D materials, van der Waals forces and π-π stacking interactions turned out to be the most popular ones to enable highly hydrophobic molecules and π-conjugated systems to interact with the basal plane of 2D surfaces.[91] The anchoring group can simply be long and linear alkyl chains, which were shown to display a high affinity for the basal plane of graphite[92] and bulk TMDs[93], or polyaromatic moieties such as a pyrene derivatives[94, 95] for physisorption on graphene and carbonaceous materials *via* π-π stacking[96].

Alongside, electrostatic interactions represent an additional class of intermolecular forces which are extremely useful for fabricating (photo)responsive hybrid systems since the anchoring group already integrates a function which can be imparted to the 2D materials, *via* local electrostatic interaction with 2D materials whose electronic properties can be mildly perturbed. Electrostatic interactions can be exploited by using molecular systems possessing full permanent charges of opposite signs, as well as hydrogen bonds involved between partially positive hydrogen atoms and highly electronegative atoms, such as nitrogen N, oxygen O and fluorine F.

By taking advantage of these characteristics, non-covalent interactions have been used for the functionalization of GRM and TMDs with light-sensitive molecules. Spiropyrans represent an important class of photochromic molecules, whose photochemical properties have been widely exploited in the last few years in order to fabricate hybrid 2D material-based devices, in particular optical switching devices. In this regard, Song et al. reported the non-covalent functionalization of solvent-exfoliated graphene *via* specifically designed perylene diimide group (PDI).[97] In this case, the photochromic spiropyran is connected to graphene through

the PDI moiety acting as anchoring group. The physical adsorption of the spiropyran-PDI dyad on graphene was monitored by means of fluorescence spectroscopy, by following the intensity of the characteristic peaks of the light-sensitive system with an increasing concentration of graphene. The results revealed a decrease in the fluorescent signals with the increasing graphene concentration. Such fluorescence quenching can be ascribed to the gradually increasing spiropyran-PDI adsorption on graphene, accompanied by a Föster resonance energy transfer (FRET) from the fluorophore to the carbon plane.[98] Ultimately, the fluorescence spectra provided more intuitive evidence for the non-covalent π-π stacking interaction, since the involvement of different types of interactions, such as electrostatic interactions, would not determine a fluorescence quenching. In this regard, an evident example has been reported by Chen et al.,[99] who studied the adsorption of cationic azobenzene molecules onto the negatively charged surface of graphene oxide (GO) nanosheets. The high fluorescence of the azobenzene-GO hybrid demonstrates that the two systems interact predominantly *via* electrostatic interactions rather than π- π stacking, which would lead to the quenching of the fluorescence. On this view, π-π interactions might be exploited to physically tether onto the surface of 2D materials possessing an extended π-conjugation such as graphene a broad range of photoresponsive molecules including spiropyran derivatives,[100, 101] metal complexes,[102] perylene diimides[82, 103, 104] and coumarin derivatives,[105] for several different applications spanning from (bio)sensing to optoelectronics. The perylene diimide derivatives have also been used as surfactants for the exfoliation of graphene nanosheets.[106] In the last few years, the non-covalent functionalization has been exploited also on 2D systems beyond graphene as well, and a prime example is represented by TMDs. The latter possess remarkable and versatile properties which can be further tuned by means of non-covalent interactions with molecular systems, and especially light-responsive ones. Indeed, unlike graphene, TMDs exhibit sizable bandgap and are promising candidates for the fabrication of electronic devices, such as FETs,

phototransistors and diodes.[11-13] Van der Waals interactions gather short-range weak intermolecular forces and have three major contributions coming from permanent dipole-dipole interactions (Keesom forces), dipole-induced dipole interactions (Debye forces) and induced dipole-induced dipole interactions (London forces). Therefore, they play a fundamental role in the functionalization of 2D crystals, especially those which do not possess π-conjugated structure such as TMDs (e.g., $MoS_2$, $MoSe_2$, $WS_2$, $WSe_2$) and black phosphorus. In particular, van der Waals interactions have been employed to anchor diazirines,[85] spiropyrans,[107] dihydroazulenes,[100] azobenzenes,[108] diarylethenes,[109, 110] perylene diimides,[111, 112] porphyrins [113, 114] and phthalocyanines,[115-118] especially metal-derivatives in the last two cases, onto the surface of 2D materials in order to obtain photosensitive hybrid systems characterized by enhanced properties and performances. Finally, the non-covalent functionalization is a smart, poorly invasive and efficient approach to combine the remarkable properties of 2D materials with the fascinating and versatile photochemistry provided by light-responsive molecular systems.

### 2.3. Covalent functionalization

To overcome the non-covalent functionalization limits (concerning the inferior robustness as well as thermal and chemical stability of the resulting hybrid systems) and even improve the results related to the formation of robust light-responsive hybrid structures, research endeavors have been devoted to the design and optimization of functionalization strategies aiming at covalently grafting photosensitive molecular systems to 2D materials. Covalent anchoring involves forces of greater magnitude with respect to non-covalent interactions, being in the range from 10 – $10^2$ kcal $mol^{-1}$, and entails the formation of a new covalent bond between the interacting species.[87] Furthermore, covalent anchoring guarantees better connectivity between the different moieties of the hybrid system, which can facilitate the charge and/or energy transfer from the photosensitive molecule to the 2D structure. A

potential drawback of covalent functionalization is the decrease of conductivity and charge carrier mobility for carbon-based materials, due to the re-hybridization of some C atoms from $sp^2$ to $sp^3$ yielding the formation of scattering centers.[88] Nevertheless, an accurate control over the degree of functionalization can minimize this issue, promoting an efficient charge transfer and limiting the effects of scattering centers.[119] Moreover, the electronic coupling between 2D materials and light-sensitive molecules through covalent bond may improve electronic cross-talk and reduce contact resistance, thus enhancing the performances of electronic devices.[120] Finally, although covalent interactions often require the use of harsh functionalization conditions (high temperature, long reaction time under inert atmosphere, etc.), undermining the compatibility with some functional groups, it guarantees a better thermal and chemical stability of the hybrid systems due to the stronger nature of the bond. Therefore, covalent anchoring has been widely used to functionalize 2D structures and exploit the inherent reactivity of the species involved in the molecular approaches. In particular, carbon-based materials and 2D GRM, namely GO, reduced graphene oxide (rGO) and graphene, have been massively employed in covalent functionalizations, especially with photosensitive molecules,[121] optimizing the molecular strategies to achieve the final hybrid systems. In this framework, a plethora of possible chemical approaches can be exploited by considering the reactivity associated to the oxygen functionalities and carbon basal plane in GRM systems. Indeed, an elegant alternative is represented by the so-called amide linkage, where the carboxylic groups present in GO and rGO are converted in the acyl-chloride derivatives *via* activation process with thionyl chloride, $SOCl_2$. In this way, the activated 2D system exhibits higher reactivity towards the reacting amino-derivatives, leading to the hybrid system by means of an amide linkage.[122] The aforementioned covalent functionalization can also take place by exploiting the direct reaction of the carboxylic groups in GO and rGO with the reacting amino-derivatives, but it envisages the use of an appropriate catalyst. In this regard, Nguyen *et al*.[123] reported on the functionalization of GO nanosheets with amino-

azobenzene molecules *via* direct amide linkage in the presence of a specific catalyst called HATU (1-[Bis(dimethylamino)methylene]-1H-1,2,3-triazolo[4,5-b]pyridinium 3-oxid hexafluorophosphate, Hexafluorophosphate Azabenzotriazole Tetramethyl Uronium), the latter being essential for generating an active ester from a carboxylic acid. Finally, another covalent anchoring strategy, less adopted but still efficient, is the one comprising the catechol chemistry, which tends to promote the formation of an ester bond when carboxylic functionalities react with hydroxyl groups under mildly alkaline conditions.[124, 125]

A pioneering work in the framework of grafting covalently small molecules to carbon nanostructures has been reported by Prato in 1993, by using 1,3-dipolar cycloaddition of azomethine ylides to covalently functionalized fullerenes by exploiting nitrogen chemistry.[126] Such an approach was then proven being of general applicability also for carbon nanotubes[127] and graphene[128]. Alongside, another strategy which is nowadays rather popular consists in the diazonium grafting of amino-derivative molecules to the basal plane of carbonaceous surfaces,[129-134] through the amino group conversion in diazo moiety *via* sodium nitrite reaction.[135, 136]

Typically, the light-responsive molecules are directly attached to the 2D crystals prior appropriate molecular designing; however, it can be also possible to resort to multi-chemical steps in order to bind the desired moiety to the system. Indeed, Wang *et al*.[137] and Yan *et al*.[138] were able to tether photosensitive molecules such as porphyrins and azobenzenes to graphene nanosheets *via* the “click” chemistry approach, by exploiting the reactivity between already immobilized acetylene groups, thanks to diazotation reaction, and azide-terminal photosensitive molecules. However, diazonium grafting is not the only option and many other strategies have been developed in order to further expand the broad range of functionalizing molecular systems.

In analogy to non-covalent approaches, covalent strategies have been developed and properly designed to functionalize other 2D materials beyond graphene, such as TMDs. Although the

scientific literature about the covalent immobilization of light-sensitive molecules on 2D systems beyond carbon-based materials is still scant, it is possible to identify and highlight a few inspiring and noteworthy works. McAdams *et al*. provided the first and prime example about the covalent functionalization of liquid-phase exfoliated $MoS_2$ nanosheets with lanthanide metal complexes, taking advantages of the varied luminescence properties of the rare earths.[139] The authors exploited metal complexes, bearing magnetic and luminescence properties based on Eu (III) and Gd (III) respectively, presenting thiol groups in the structure in order to use the latter as anchoring group to fill sulfur vacancies present in the crystal lattice, leading to multimodal hybrid systems.[140] Additional strategies to bind light-sensitive molecules to 2D platforms exploit either the diazonium grafting on $MoS_2$ substrates[141] or the direct functionalization of $MoS_2$ basal plane by means of organohalides[142], both followed by chemical approaches, such as "click" chemistry reactions,[143] to form photosensitive systems.[144]

By and large, covalent anchoring is a promising, versatile and efficient strategy to functionalize 2D materials and finely tune the properties of the resulting hybrid systems, as demonstrated below.

## 3. Tunable optical response of 2D materials by molecular functionalization

Two-dimensional materials have shown remarkable optical properties which are markedly different from those of their bulk (multilayer) counterparts. For example, group-6 TMDs are indirect bandgap semiconductors in their bulk form and converted to direct bandgap in their monolayer limit.[145, 146] Because of this reason, the PL of monolayer TMDs is greatly enhanced and several unique optical properties can be accessible for investigation, such as strong excitonic effect, spin- and valley-dependent optical response.[8, 147] Moreover, the surface functionalization by light-sensitive molecules will effectively modulate the optical properties of 2D materials due to their high environmental sensitivity.

The interaction between 2D materials and photochromic molecules can be classified into two mechanisms, which is dipolar interaction and charge transfer. For azobenzenes and spiropyrans (**Figure 3**a and 3b), the two isomers exhibit a sizable change in the dipole moment.[39, 148] Conversely, for diarylethenes (Figure 3c), the conversion between open and closed form greatly alters the energy level of the molecular orbitals, which can lead to an effective tuning of the band alignment in the molecule/2D hybrid system thereby affecting the charge transfer.[149] Other photo-sensitive molecules, such as chromophores, can absorb the light with a certain wavelength based on the energy band diagram and then interact with adjacent layers to induce the change of optical properties.[150] Dipole interaction works as an external electrostatic gate to manipulate the carrier density of the underlying 2D semiconductors, being a universal method to optically switch 2D electronics. Conversely, the charge transfer requires the appropriate band alignment between molecules and 2D layers to realize light-controlled 2D devices. In this section, we will focus on the tunable PL and photoresponse properties of 2D materials functionalized with light-sensitive moieties.

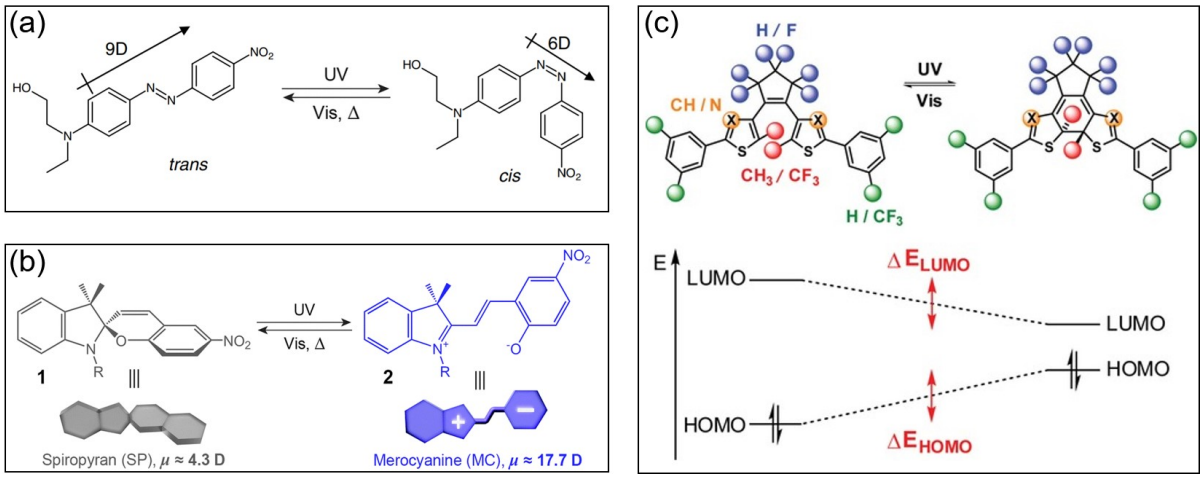


**Figure 3.** Photoisomerization of (a) azobenzene, (b) spiropyran, and (c) diarylethene. The main distinctive properties of the two isomers have also been highlighted. (a) Adapted with permission.[148] Copyright 2007, American Physical Society. (b) Adapted under a Creative Commons Attribution 3.0 Unported Licence.[39] Copyright 2014, Royal Society of Chemistry. (c) Adapted with permission.[149] Copyright 2017, Wiley-VCH.

### 3.1. Photoluminescence

The PL emission in semiconductors results from the electromagnetic radiation with specific energy and it is determined by the radiative recombination of excitons. The emission wavelength is strongly dependent on the electronic band structure. As a model 2D semiconductor, monolayer $MoS_2$ has been extensively studied for its fundamental optical properties and the potential application in optoelectronic devices. The PL of monolayer $MoS_2$ is dominated by the direct transition between valence and conduction band states around K and K' points (**Figure 4**a).[151] The large spin-orbit interaction splits the highest valence bands at the K (K') point by ~150 meV.[152] Figure 4b shows the representative PL spectra of monolayer $MoS_2$ on $SiO_2$/Si substrate, which has two dominant peaks A and B. They correspond to the recombination of excitons at the lowest conduction bands and the highest spin-split valence bands. For the A peak, it is composed of the neutral A exciton and the negatively charged $A^-$ trions (a quasiparticle, composed of two electrons and a hole), as shown in Figure 4c.[153] Mak *et al.* adopted an electrostatic-gating method to tune the carrier density of $MoS_2$ (Figure 4b).[151] When the electron density is large, the PL peak A is dominated by the trion emission due to the great suppression of neutral exciton recombination. With the decreasing electron density, the spectral weight of neutral exciton emission increases dramatically. Therefore, by tuning the carrier density, it is feasible to manipulate the PL emission of monolayer $MoS_2$.

Photochromic molecules offer a unique way to modulate the carrier density of $MoS_2$ and the PL spectra *via* the optical remote control. Li *et al.* reported the tunable PL spectra of monolayer $MoS_2$ placed on self-assembled monolayers (SAMs) of photoswitchable azobenzene molecules.[108] The azobenzene molecules, exposed at the extremity of an alkylthiol (molecular structure in Figure 4d) were first self-assembled on the Au coated quartz substrate and then mechanically exfoliated $MoS_2$ flakes were transferred onto the top of the molecules (Figure 4d). The photoisomerization of azobenzenes could be triggered by the UV and visible light irradiation. When the molecules were in their *trans* form, the extra electrons

in $MoS_2$ suppressed the PL emission of neutral A exciton, which resulted in the low PL intensity. After the molecules switch to *cis* form, the PL intensity showed a clear three-fold enhancement (Figure 4e).[108] The authors also performed Kelvin probe force microscopy (KPFM) measurements to confirm the relationship between molecular switching and the work function shift of this hybrid system. When switching from *trans* to *cis*, the surface potential of the system decreases, indicating the increase of the work function, thus *p*-doping the 2D material. The decreasing electron density resulted in the enhanced PL emission. Upon the design and use of an *ad hoc* azobenzene derivative (e.g. being electronegative or electropositive), the magnitude of the work function of the hybrid system could be tuned in a large range, and thereby providing a great degree of remote control on the PL spectra of $MoS_2$ flakes.

Alongside the tuning of the PL by using the isomerization of photochromic molecules as remote control, lanthanide complexes with attached organic ligands can also be adopted to functionalize 2D layers and modulate their PL spectra. A representative example consisted in the covalent functionalization of Eu (III) complex on $MoS_2$ surface to form a novel 2D luminescent material.[139] The hybrid system preserves the 2D structure and the sensitized luminescence from $Eu^{3+}$. The $^5D_0 \rightarrow {}^7F_J$ (J=0,1,2,3,4) emission line of $Eu^{3+}$ can be observed on $Eu^{3+}$ functionalized $MoS_2$ with sharp line-like peak and long lifetime. These unique optical properties can be used in optical and biological imaging. With this successful attempt, the authors further managed to functionalize $MoS_2$ sheets with both Eu (III) and Gd (III) complex, exhibiting luminescent (millisecond lifetime) and paramagnetic properties.[139] In this way, the physical properties of $MoS_2$ sheets could be adjusted through the designed molecular functionalization.

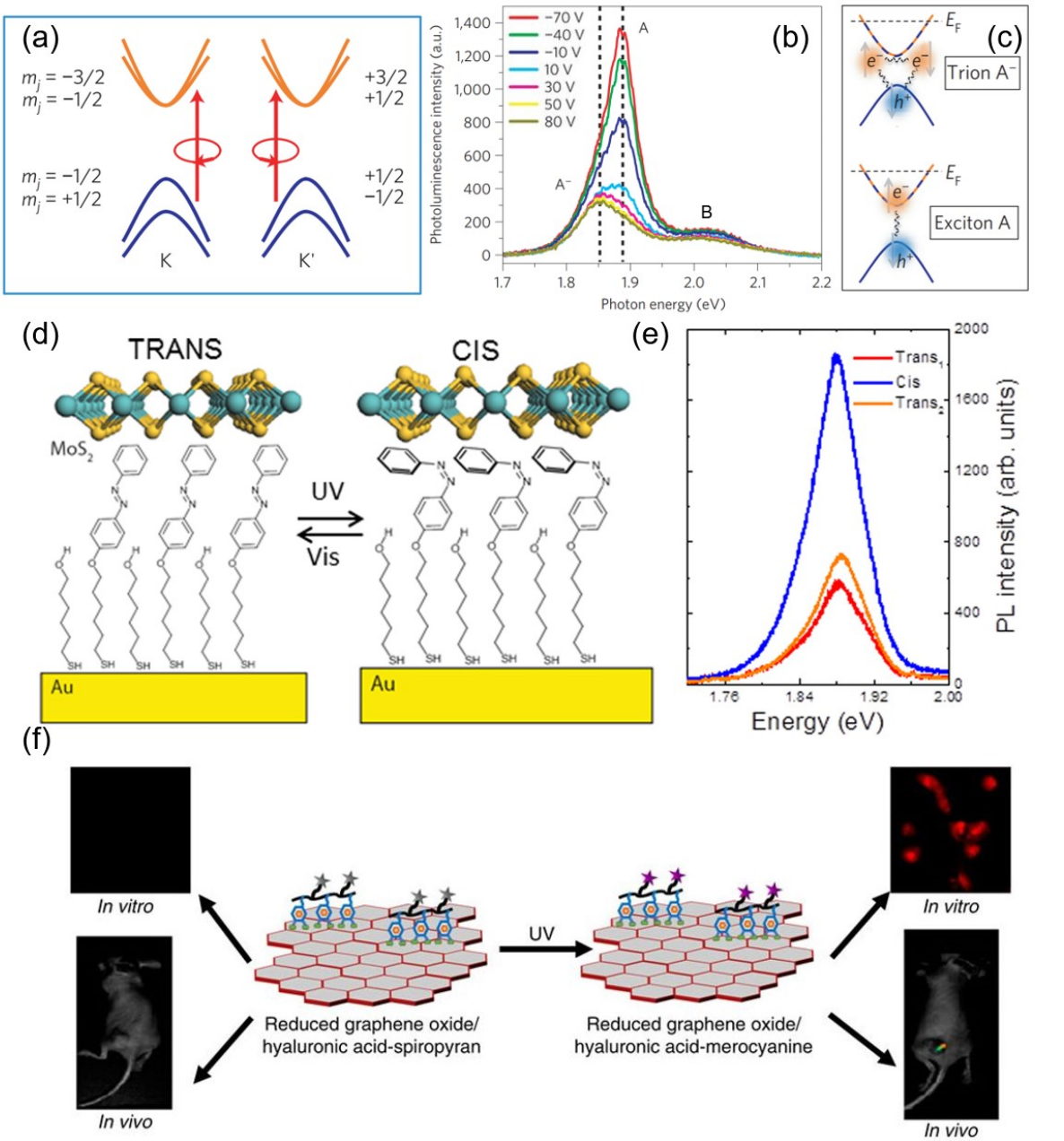


**Figure 4.** (a) Simplified band structure of monolayer $MoS_2$ at K and K' point. The spin-orbit coupling induces the splitting highest-energy valence bands. (b) The photoluminescence spectra of monolayer $MoS_2$ at different back-gate voltages. The neutral A exciton, the negative $A^-$ trion, and B exciton are indicated in the spectra. Adapted with permission.[151] Copyright 2012, Nature Publishing Group. (c) The schematic of the neutral A exciton and negatively-charged $A^-$ trion. Adapted with permission.[153] Copyright 2012, American Chemical Society. (d) The schematic of $MoS_2$/azobenzene/Au hybrid system. The monolayer $MoS_2$ is exfoliated onto the self-assembled monolayers of azobenzene molecules. (e) The photoluminescence of monolayer $MoS_2$ tuned by the isomerization of azobenzene molecules. Adapted with permission.[108] Copyright 2014, American Institute of Physics. (f) rGO/hyaluronic acid-spiropyran used for in vivo fluorescence imaging. Adapted with permission.[125] Copyright 2013, American Chemical Society.

While in its pristine form, as a result of the absence of a bandgap, graphene does not emit light, when defects are introduced in the 2D lattice such a property is recovered. This is the

case of GO and rGO, whose defect-rich nature can render them fluorescent. Due to the diverse oxygen groups (such as epoxy, hydroxyl, and carboxyl) intrinsically incorporated in their structure which include some independent fluorophores, GO and rGO shows versatile fluorescent spectra over a broad spectral range. Nahain *et al.* reported the chemical functionalization of rGO with spiropyrans yielding tunable fluorescent nanosheets.[125] The functionalized rGO sheets retain the photochromic features and display yellow to purple color change after the photoisomerization from the spiropyran to merocyanine form. The in vitro and in vivo fluorescence image tests demonstrated that the nanosheets can be used as a fluorescent probe for diagnosis (Figure 4f).[125]

Overall, through the functionalization of 2D layers by photosensitive molecules, the PL of the hybrid systems can be effectively tuned in a controlled way. Such hybrid systems are promising for applications as biological markers and light-emitting system as well as for being integrated in light-sensitive optoelectronic devices.

### 3.2. Photoresponse properties

2D materials exhibit distinct photo-responsive performance with varied detection range. Graphene, with its gapless and linear-dispersion electronic structure, shows a broadband photodetection from UV, visible, infrared and up to terahertz (THz) spectral regimes.[154] Monolayer graphene absorbs 2.3% of the incident light, independently on the wavelength. Although this value is remarkably high for a sub-nanometer thin layer, it is very small in absolute terms, which limits the photoresponsivity of graphene photodetectors.[155, 156] The charge-transfer-assisted photodetection is the most commonly adopted method to overcome this issue, by fabricating a hybrid system, composed of 2D materials and optically active molecules.[154, 157] The electron-hole pairs are generated in both 2D materials and active molecules under light irradiation. One type of carrier in molecules can be transferred to 2D layers, driven by a built-in electric field at the interface. The transferred carriers increase the

carrier density of 2D layers and result in the enhancement of photocurrent. However, to increase the photocurrent, the photoresponsive speed is inevitably sacrificed. The opposite carriers in the active components reduce the recombination rate, increase the carrier lifetime, and unfortunately decrease the photoresponse speed. Therefore, these photodetectors can be used in video imaging applications, which require high spatial and low temporal resolution.

Zhang *et al.* reported azobenzene-functionalized GO with improved photoresponse properties.[122] The azobenzene groups were covalently bonded on the edge of GO as shown in **Figure 5**a. The XPS analysis revealed a degree of functionalization of ~1 azobenzene chromophore each 55 carbons of GO.[122] The fluorescence spectra of azobenzene/GO were strongly quenched compared with azobenzene samples, due to the photoinduced electron transfer from the azobenzene chromophore to the GO sheets. But the photoresponse of azobenzene/GO was greatly enhanced with the increasing photocurrent (Figure 5b). The ratio of photocurrent under UV irradiation vs that under dark was as high as ~800%.[122] The light irradiation resulted in a charge transfer from photoexcited singlet azobenzene moieties to the conduction band of GO, due to the appropriate band alignment of the azobenzene/GO hybrid system. The fast charge transfer within the intramolecular donor-acceptor system gave rise to the large photocurrent.

Besides photochromic molecules, the functionalization of graphene layers with dyes can also greatly enhance the photoresponse of the hybrid system. The graphene sheets were covalently functionalized with zinc porphyrin and ruthenium phenanthroline, respectively.[137] The measured photocurrent from the hybrid system showed great enhancement due to the stable charge transfer from the photoactive groups to the graphene sheets under illumination. Wieghold et al. reported a bicomponent supramolecular H-bonded network, consisting of a terrylene diimide derivative and melamine, assembled on graphene surface, which showed apparently high photocurrent and photovoltage.[83] The devised approach represents a novel self-assembled method to fabricate monolayer/thin-layer sensitizers in optoelectronics devices.

Alongside, three-dimensional ordered GO layers functionalized with common redox-active dyes, including an anionic Zn(II) phthalocyanine derivative, a cationic porphyrin and a cationic perylene diimide derivative, were obtained through electrostatic interaction in water.[81] The GO composite effectively absorbs the light from UV to near-infrared range due to the nonoverlapping absorption maxima of the three molecules and exhibits the higher photocurrent density when compared to only GO or dye molecules. This is due to the strong interaction between molecules and the GO surface, and the ultrafast charge separation process with Zn(II) phthalocyanine derivative and perylene diimide derivative as the ultimate electron donor and acceptor, respectively. One promising application of these hybrid systems is to facilitate photoelectrochemical water splitting. Balapanuru et al. reported the functionalization of rGO with perylene dye and Co(II) ions.[82] The efficient light absorption of perylene dye, the electrocatalytic activity of Co ions and the ultrafast charge transfer from dye molecules to rGO together contribute to the high performance of hydrogen evolution reaction.

TMDs with suitable bandgap have been explored as the photodetector for visible and near-infrared light.[158] In order to increase the photocurrent and even extend the photoresponse range, photoactive molecules can be employed to functionalize the TMDs flakes, such as organic dye molecules. Huang *et al.* prepared the $MoS_2$ photodetector *via* the physisorption of three dye molecules (Figure 5c), i.e. methyl orange, rhodamine 6G, and methylene blue.[27] The different photodetector performances were observed on the three devices due to the variation of molecular structure and extinction coefficients. The hybrid methylene blue/$MoS_2$ photodetector showed the best performance, characterized by a ~19 times larger photocurrent than that of pristine $MoS_2$ (Figure 5d). Compared with the other two molecules, the flat molecular structure and the excellent light absorption ability facilitated the charge transfer of photoexcited electrons from the methylene blue molecules to the monolayer $MoS_2$ (Figure 5e). Yu et al. reported that rhodamine 6G can not only increase the photocurrent, but also extend the photodetection range to the near-infrared (from 980 nm to 405 nm). The wide infrared

detection is due to the photoinduced electron transfer from HOMO of rhodamine 6G to the bottom of $MoS_2$ conduction band.[159] Therefore, the dye molecules with the function of the synergistic light absorption led to the improved hybrid $MoS_2$ photodetector performance. The methylene blue molecules can be also used as photosensitizer, which can produce singlet oxygen under light exposure with specific wavelength to kill the nearby cells. The liquid-exfoliated $WS_2$ nanosheets with large surface area can carry photosensitizers (methylene blue) for photodynamic therapy. Together with the near-infrared absorption properties and strong X-ray attenuation ability of $WS_2$, the hybrid methylene blue/$WS_2$ system represents a multifunctional platform for imaging and therapy.[160]

Alongside the dye molecules, some molecules containing chromophoric groups can also affect the photoresponse of TMDs. Zinc-centered protoporphyrin IX (ZnPP) was physisorbed on the surface of liquid-exfoliated group-6 TMDs.[113] The photoelectrochemical measurements demonstrated two distinct photoresponse phenomena after functionalization, showing positive photocurrent for disulfides compounds and negative photocurrent for diselenides compounds. By comparing HOMO/LUMO levels of ZnPP molecules with the band energies of group-6 TMDs, two charge transfer paths have been proposed, i.e. the transfer of photo-excited electrons from ZnPP to disulfides and the transfer of photo-excited holes from ZnPP to diselenides, respectively. Similarly, different photocurrent modulations were observed in $MoS_2$ and $MoSe_2$ flakes after functionalization with perylene diimide derivative.[111] Therefore, the combination of TMDs materials with light-sensitive molecules will contribute to distinct photoresponse *via* the proper design of the band alignment.

Overall, the photoresponse of the 2D materials can be greatly enhanced through the functionalization with photoactive molecules due to the photo-induced charge transfer process. Future works should be focused on improving the photoresponse speed to expand the applications of the hybrid photodetector devices.

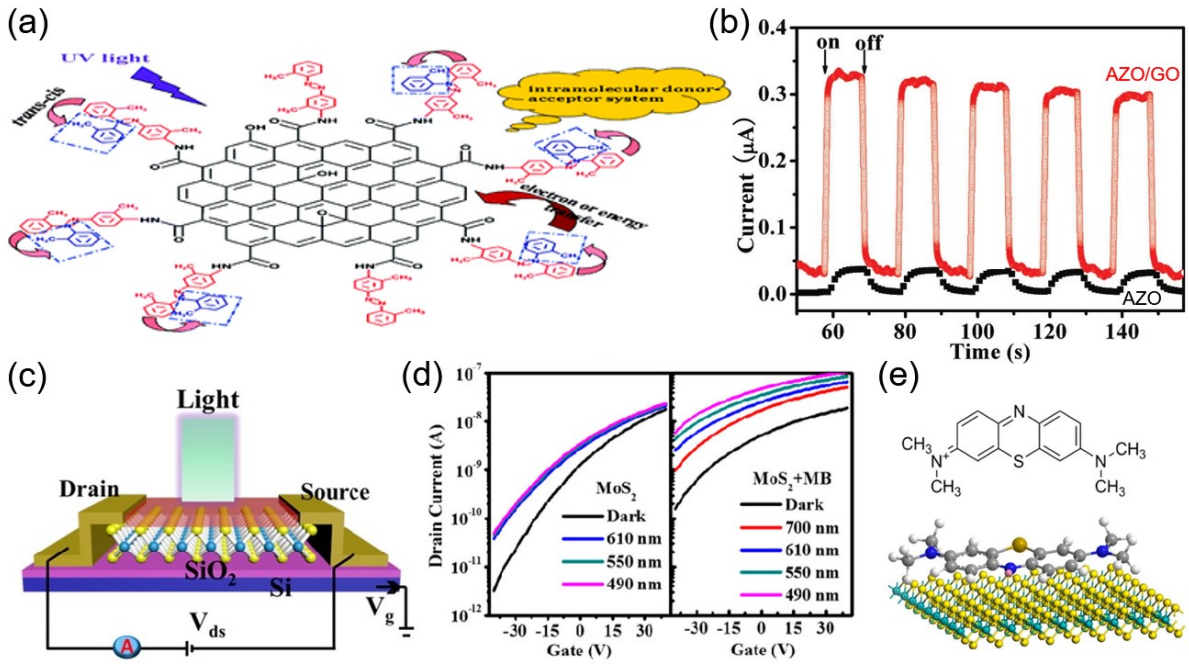


**Figure 5.** (a) The schematic of the chemical functionalization of graphene oxide with azobenzene. (b) Photocurrent response of the pristine azobenzene and azobenzene/GO film, respectively. Adapted with permission.[122] Copyright 2010, American Chemical Society. (c) Schematic of the photodetector (or phototransistor) structure. (d) The transfer curves of the pristine $MoS_2$ FET and $MoS_2$ FET with methylene blue (MB) functionalization under different light irradiation conditions. (e) Molecular structure of methylene blue and the optimized structure of the hybrid MB/$MoS_2$ system with minimized energy. Adapted with permission.[27] Copyright 2016, American Chemical Society.

## 4. Optically controlled 2D electronic devices *via* the functionalization with photochromic molecules

The applications of 2D materials in electronic and optoelectronic devices have been the subject of intensive research aimed at taking advantage of their atomic-level thickness, high carrier mobility, excellent electrostatic control with reduced short-channel effect, and unique optical response.[161-164] In addition to these bonuses, in order to achieve light-responsive electrical transport one viable route consists in the construction of novel devices integrating the functions of photochromic molecules and 2D layers. The photochromic molecules can be anchored to the surface of 2D materials either non-covalently or covalently. **Table 3** summarizes the optically switchable doping effect on 2D materials conferred by photochromic molecules by highlighting the thickness of the 2D layers, the functional groups

responsible for molecule/2D interaction, interaction mechanism and the carrier density change *via* the isomerization of molecules. In the next subsections, we will systematically discuss the light-controllable electronic devices based on the hybrid system (photochromic molecules/2D layers), with a special focus on applications in optically controlled logic devices, memory devices, and energy-related devices.

**Table 3.** Optically-switchable doping effect on 2D materials by photochromic molecules.

| 2D material | Thickness | Molecule | Interaction group | Bond type | Interaction mechanism | $\Delta n$ ($cm^{-2}$) | Note | Ref. |
|---|---|---|---|---|---|---|---|---|
| Graphene | Monolayer | AZO | diazonium | Covalent | DI | $3\times10^{11}$ | | [133] |
| Graphene | Bilayer | AZO | diazonium | Covalent | DI | $3.6\times10^{11}$ | | [133] |
| Graphene | Trilayer | AZO | amide | Covalent | DI | $4.4\times10^{13}$ | GO | [123] |
| Graphene | Monolayer | AZO | pyrene | Non-covalent | DI | $8\times10^{11}$ | | [165] |
| Graphene | Few layer | AZO copolymer | | Non-covalent | DI | $7.2\times10^{11}$ | | [166] |
| Graphene | Monolayer | AZO | | Non-covalent | DI | $1\times10^{13}$ | Irradiation method 1 | [167] |
| Graphene | Monolayer | AZO | | Non-covalent | DI | $4.7\times10^{13}$ | Irradiation method 2 | [167] |
| Graphene | Monolayer | SP | Alkyl chain | Non-covalent | DI | $4.4\times10^{12}$ | | [107] |
| $MoS_2$ | Monolayer | SP | Alkyl chain | Non-covalent | DI | $4.6\times10^{12}$ | | [107] |
| Graphene | 2-bilayer | SP | pyrene | Non-covalent | DI | $8.13\times10^{11}$ | GO | [168] |
| Graphene | 5-bilayer | SP | pyrene | Non-covalent | DI | $2.95\times10^{11}$ | GO | [168] |
| Graphene | Monolayer | SP | pyrene | Non-covalent | DI | $4.68\times10^{11}$ | | [101] |
| Graphene | Monolayer | DAE | | Non-covalent | CT | | supercapacitor | [110] |

Note: AZO, azobenzene; SP, spiropyran; DI, dipole interaction; GO, graphene oxide; irradiation method 1: UV irradiation after molecular deposition; irradiation method 2: UV irradiation during the molecular deposition. DAE, diarylethene; CT, charge transfer.

### 4.1. Field-effect transistors

A transistor is the prototypical building block and active component in all modern electronics. The demand for increasing the number of transistors per unit area in tomorrow's integrated circuits, requires the further reduction of the transistor size, reaching the limit of nowadays Si

technology. In this framework, 2D materials have been regarded as the promising candidate to replace Si as channel materials. 2D materials provide the opportunity to design ultrathin channel transistors with improved gate control and low power consumption.[17, 169] The diverse physical properties of 2D materials enable their use as transparent electrodes, channel materials, and the dielectric layer.[170] Graphene FET shows ultrahigh carrier mobility, but very small $I_{on}/I_{off}$ ratio due to the absence of a bandgap.[171, 172] Recently, graphene has been widely used as electrode for devices comprising 2D semiconductors as active materials.[173] TMDs with a thickness-dependent bandgap have been widely explored as channel materials with large $I_{on}/I_{off}$ ratio and sizable carrier mobility.[174-176] After the functionalization with photochromic molecules, the work function of graphene and the carrier density of TMDs can be effectively tuned by remote optical control. These unique features can be adopted to design novel functional devices.

In conventional back-gated FET structure, 2D materials are electrically connected with top metal contacts and the channel area is exposed for functionalization. Gobbi *et al.* designed and synthesized the spiropyran derivative terminated with an 18-carbon long alkyl chain.[107] The long alkyl chain promotes the formation of physisorbed crystalline self-assembled monolayers (SAMs) of molecules on graphene and $MoS_2$ surface. The authors correlate the molecular-level control of the superlattice with the electrical transport in the device scale. They find that after the UV irradiation, both graphene and $MoS_2$ FETs show *n*-type doping effect with the shift of the charge neutrality point and the threshold voltage, respectively (**Figure 6**a and 6b).[107] The induced electron density in monolayer graphene and $MoS_2$ is as large as 4.4 and 4.6 × $10^{12}$ $cm^{-2}$. The ex-situ scanning tunneling microscopic (STM) images exhibit apparent structural changes (shortening the long side and elongating the short side) after the photoisomerization from spiropyran to merocyanine form (Figure 6c and 6d). The area of the unit cell increases from 2.5 $nm^2$ to 4.7 $nm^2$. The theoretical calculation confirmed that the two isomers show distinct molecular electrical dipoles perpendicular to the surface ($\mu_z$

= 0.23 and 1.7 D per spiropyran and merocyanine molecule, respectively). The polarization induced by the molecular dipoles, acts like an external electric gate, yielding a shift of the work function and inducing a doping effect. Therefore, the light-induced structural reorganization of the SAMs on the 2D surface directly leads to the change of the carrier density in 2D layers.

The presence of an ordered supramolecular array of photochromic molecules on the top of the 2D materials is a viable strategy to harness the doping effect. Yet, despite with a reduced magnitude, such a doping can be also attained upon physisorption of photochromes forming less ordered adlayers. Representative examples are those of pyrene-modified azobenzenes and spiropyrans physisorbed on graphene surface *via* π-π interaction.[101, 165, 168] Despite the random distribution of photochromic molecules on the graphene surface, the change in the dipole moment of molecules triggered by light stimuli, can affect the local electronics of the 2D material underneath. In particular, the shift of Dirac point in the electrical measurement demonstrated the reversible doping effect in monolayer graphene resulting from the photo-isomerization of azobenzenes or spiropyrans. The time-dependent conductance measurement clearly showed the optically switching behavior, evidenced by the current of the hybrid graphene/azobenzene system displaying repeatable increasing and decreasing cycles under alternative UV and visible light irradiation (Figure 6e).[165] The *cis*-azobenzene induces hole doping with the density of $0.8 \times 10^{12}$ $cm^{-2}$, and the electron doping density from the merocyanine amounts to $0.5 \times 10^{12}$ $cm^{-2}$. Compared with the ordered physisorbed SAMs of spiropyrans reported by Gobbi *et al.*,[107] the random adsorption of spiropyrans showed a smaller modulation range of the carrier density of graphene. Therefore, it is crucial to design the photochromic molecules with the large change of the vertical dipole moment. The Raman spectroscopy has been demonstrated as a versatile tool to correlate the crystallinity of 2D materials with the electronic properties, enabling also to unravel the effect of various perturbations on the electronic of 2D materials, such as doping, strain, and defects.[177] The

shift of the Fermi energy induced by carrier doping can change the equilibrium lattice parameter with a consequent stiffening/softening of the phonons.[178] The Raman spectra of both graphene/azobenzene and graphene/spiropyran hybrid system provided clear evidence for the reversible doping effect.[101, 165, 167] After UV irradiation, the G band of graphene showed a redshift and then after visible light irradiation, the peak returned to the original position (Figure 6f).[167] The control experiments on pristine graphene and pyrene/graphene excluded the influence of outer environment and verified the key factor of photochromic molecules. The doping results from Raman spectroscopy were also consistent with that from the electrical measurements. As the number of graphene layer increases, the photochromic molecules exhibited reduced influence on the carrier density modulation, demonstrating the short-range nature of the effect.[168]

Although the chemisorption unavoidably introduces structural defects on 2D monolayers and induces the performance degradation of monolayer 2D devices, this strategy is useful for the covalent functionalization of multilayer graphene and GO.[123, 133] While the top (or bottom) layer can act as the anchoring platform for molecules, the other inner layers (when dealing with a multilayer system) contribute to the electrical transport. Azobenzene functional groups have been functionalized on the surface of trilayer GO and bilayer graphene. Both these hybrid systems exhibit optically switchable FET behaviour.[123, 133] In particular, the hybrid bilayer graphene FET shows high light-induced resistance modulation (up to 46%) and negligible conductivity/mobility degradation.[133] Together with the robust and stable nature of chemisorption, the covalent functionalization of multilayer graphene by photochromic molecules is a promising method to fabricate optically switchable 2D FET.

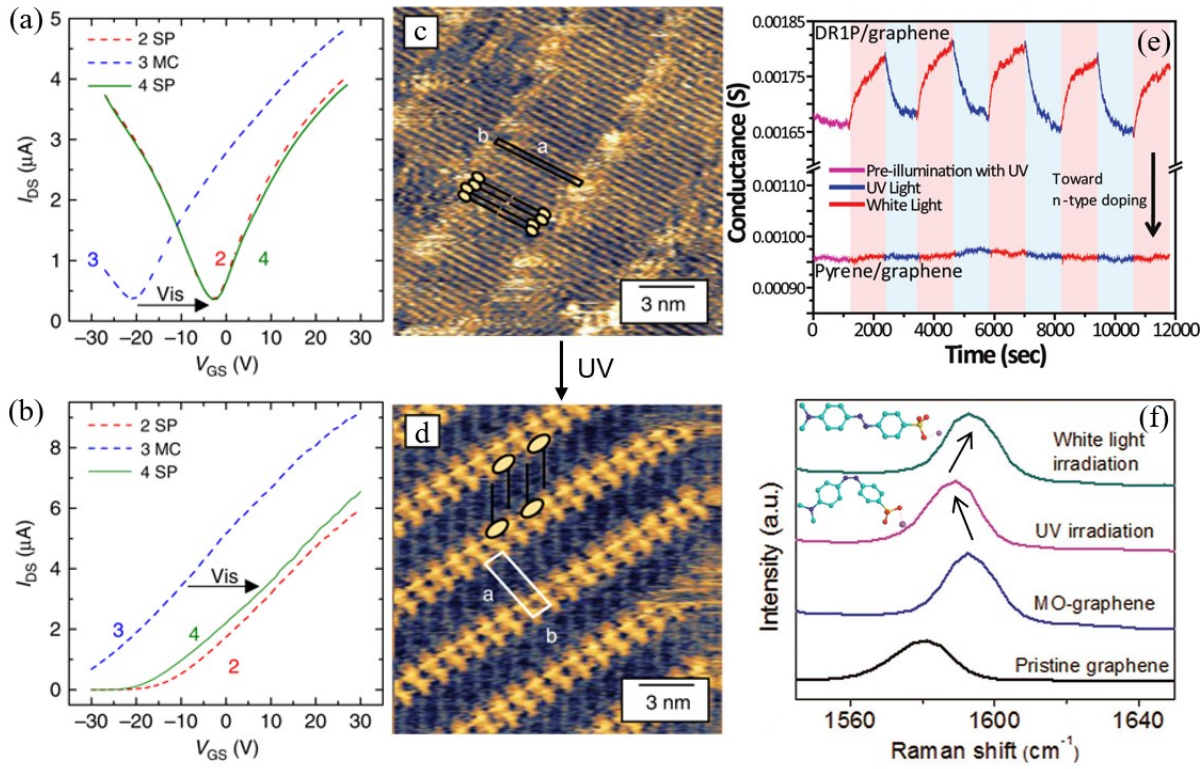


**Figure 6.** The transfer ($I_{DS}$-$V_{GS}$) characteristics of FET devices based on (a) graphene/spiropyran, and (b) $MoS_2$/spiropyran superlattice showing light-switchable electrical behavior. Scanning tunneling microscopy imaging of spiropyran assemblies on highly oriented pyrolytic graphite (HOPG). Height images of the molecular assemblies obtained (c) after spin-coating the spiropyran solution and (d) immediately after UV irradiation. A schematic sketch of the molecule is superimposed to the images to facilitate the visualization of the molecular ordering. Adapted under the terms of a Creative Commons Attribution 4.0 International license.[107] Copyright 2018, Nature Publishing Group. (e) Time-dependent conductance measurement of graphene/azobenzene transistor at 0 V gate bias. Adapted with permission.[165] Copyright 2012, American Chemical Society. (f) Raman spectra of the G band of pristine graphene, hybrid graphene/azobenzene system, UV-irradiated hybrid system, and hybrid system upon white light illumination. Adapted with permission.[167] Copyright 2012, American Chemical Society.

### 4.2. Diodes

A diode is a fundamental element that can be used to construct complex electronic circuitries. It is a two-terminal electronic device that allows current to flow in one direction yielding asymmetric conductance. Recently, diodes fabricated with 2D materials have been extensively studied due to their potential application in current rectifiers, logic gates, solar cells, etc.[13, 179-182] The common diode structure consists of a junction, such as a semiconductor-metal junction (Schottky diode) or a *p*-*n* junction (*p*-*n* diode). The Schottky

diode can be fabricated by the vertical stacking of 2D semiconductor sandwiched between metal electrodes. For example, when the *n*-type semiconductor comes in close contact with the metal layer at zero bias, the Schottky barrier height, $\Phi_B$, is the difference between the interfacial conduction band edge $E_c$ and Fermi level $E_F$. When the barrier $\Phi_B$ is low, the current can flow in both directions forming the ohmic contact, otherwise, the current will show the rectifying characteristics due to the high barrier for electrons to overcome. The adsorption of photochromic molecules is a feasible method to effectively tune the doping concentration and Fermi level of the 2D semiconductors. Therefore, it is possible to construct an optically switchable Schottky diode by using photochromic molecules to functionalize 2D semiconductors and modulate the barrier height $\Phi_B$ of the semiconductor-metal junction.

Margapoti *et al.* reported a photoswitchable diode, composed of a 2D $MoS_2$ layer on top of a mixed chemisorbed monolayer, of thiolated azobenzenes in an alkanethiol matrix, assembled onto a gold electrode (**Figure 7**a).[183] The electrical transport tests relied on the measurement of the current passing through the vertical junction based on conductive atomic force microscopy (AFM) set up operating with a Pt-Ir tip acting as counter-electrode. The representative *I-V* curves displayed in Figure 7b revealed light-tunable transport characteristics. The current rectification can be observed on $MoS_2$/*trans*-SAM heterostructure with a turn-on voltage close to 0.5 V. After irradiating the device with UV light, the current rectification has been completely suppressed and the current density in forward bias is around 1.5 orders of magnitude larger than that in the *trans* form. Finally, the rectification behavior can be switched back by white light irradiation. In order to investigate the light-tunable mechanism, several blank tests with different channel monolayers have been conducted. When replacing $MoS_2$ (semiconductor) with graphene (semimetal), no current rectification behavior can be observed, which demonstrates the exclusive property of $MoS_2$ junction. When 2D layer is removed and only photochromic (mixed) molecular monolayers are sandwiched between the electrodes, the different tunneling currents (dependent on the

molecular length) in *trans* and *cis* form can be observed without rectification.[184, 185] The contact potentials, thus Schottky barriers, of $MoS_2$/Pt-Ir electrode on *trans*-SAM/Au and *cis*-SAM/Au are measured by KPFM, which are 1.03 V and 0.67 V, respectively. Therefore, the main mechanism responsible for photoswitchable rectification is the tunable metal-semiconductor junction between $MoS_2$ and Pt-Ir electrode. Figure 7c shows the band alignment of the metal-semiconductor junction. For the high Schottky barrier in $MoS_2$/*trans*-SAM heterostructure, it requires a large bias voltage to overcome the misaligned transport channel at both polarities. In contrast, the transport channel of $MoS_2$/*cis*-SAM is close to the work function of the metal electrode, which facilitates the electron transport at any bias. This study opens a new research area based on the combination of approaches belonging to molecular electronics and to 2D electronics with the ultimate goal of realizing photoswitchable electronics circuits and logic gates.

Another common diode architecture is the *p*-*n* junction, which can be realized either in a 2D homostructure (based on a single 2D materials) and 2D heterostructure (junction between two different 2D materials). The latter mostly concerns the well-established approaches of van der Waals vertical heterostructures.[186] Conversely, in 2D homostructure, the carrier type is controlled by the electrostatic or chemical doping in different regions of the same 2D crystal.[180, 187-191] The chemical doping can be achieved by the adsorption of molecules, nanoparticles or quantum dots on the surface. A viable method to develop photoresponsive 2D homojunctions relies on the use of adlayers of photochromic molecules acting as dopant. In this context, Gobbi *et al.* fabricated the graphene/spiropyran superlattice and controlled the local charge carrier density with high spatial resolution.[107] The authors first converted all the spiropyran molecules to the merocyanine form by UV light irradiation and then irradiated the green light only on a spatially confined region of the flake by using a focused laser (Figure 7d). Due to the presence of both spiropyrans and merocyanines on the flake, the carrier density of graphene shows a large difference in the lateral direction, which results in a 2D

homojunction. The merocyanines induce strong n-type doping, while spiropyrans only induce slight n-type doping. The electrical transport behavior of the homojunction (Figure 7e) shows a current plateau when the back-gate voltage is between -15 V to -5 V. In this back-gate voltage range, the carrier type of graphene/spiropyran and graphene/merocyanine is hole and electron, respectively. Hence, a graphene *p-n* junction can be formed. By following this methodology, 2D semiconductors featuring ambipolar transport behavior, which are commonly used in *p-n* junctions, such as $WSe_2$ and black phosphorus (BP), can be adopted in the future to fabricate the light-tunable *p-n* junction with micrometric resolution. The hybrid p-n junctions, formed by vertical stacking of semiconducting organic molecules and 2D materials (for example, p-type Cu-phthalocyanine and n-type $MoS_2$)[192], represent another concept to build diode devices. One can foresee future efforts devoted to the incorporation of photochromic groups in organic molecules *via* ad hoc design to realize light-controlled diodes.

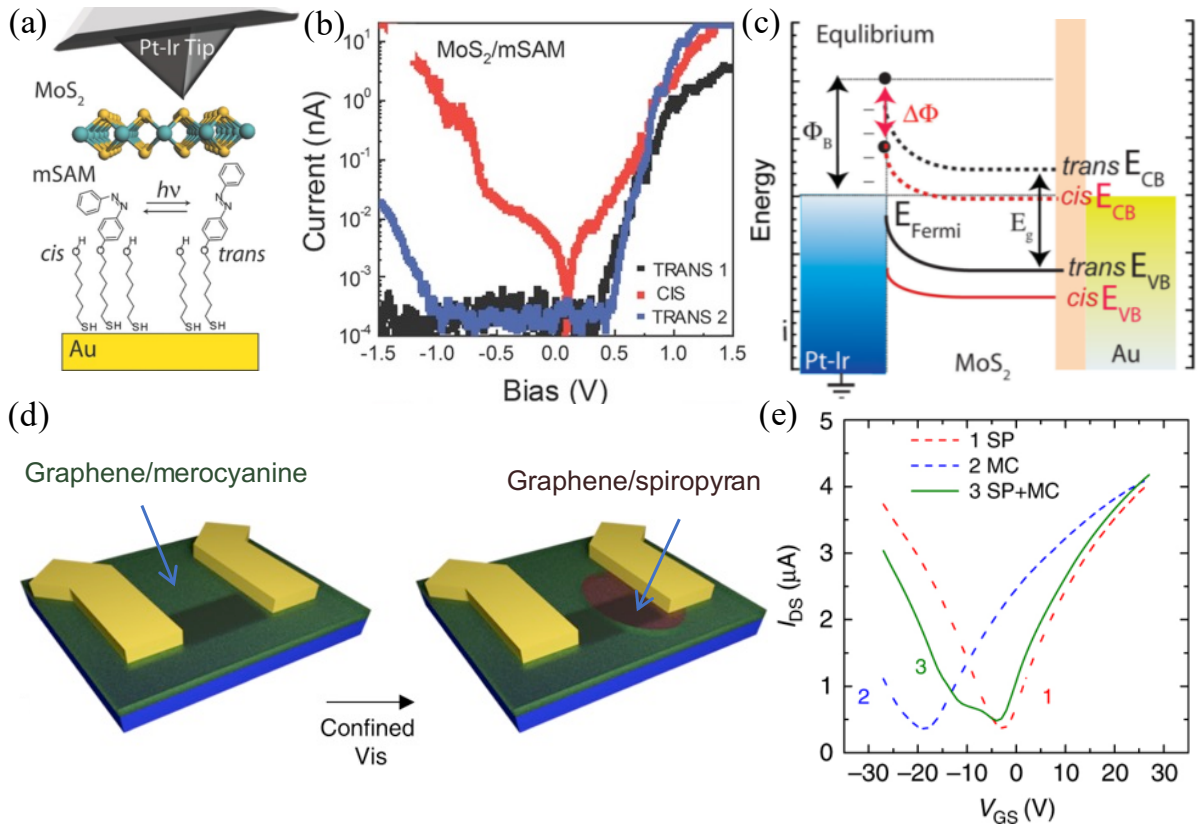


**Figure 7.** (a) Schematics of the photoswitchable diode structure. Monolayer $MoS_2$ is mechanically exfoliated on the top of a mixed SAM made of spacer molecules and

azobenzene derivatives on the gold substrate. (b) Representative *I-V* characteristics for $MoS_2$/SAM heterostructure before (trans 1), after UV (cis) and after white light exposure (trans 2). (c) Schematics of the metal-semiconductor junction between the grounded Pt-Ir tip and the $MoS_2$/SAM Au heterostructure. Adapted with permission.[183] Copyright 2015, Wiley-VCH. (d) Schematics of the photoswitchable homojunction *via* spatially confined doping based on graphene/spiropyran superlattice. The green light irradiation in a well-defined area of the channel can trigger the merocyanine to spiropyran isomerization. (e) The transfer characteristics ($I_{DS}$-$V_{GS}$) of devices based on graphene/spiropyran superlattice. Trace 1 (red): graphene covered by the spiropyran layer, trace 2 (blue): graphene/merocyanine as the channel, trace 3 (green): graphene homojunction with merocyanine and spiropyran on different channel section. Adapted under the terms of a Creative Commons Attribution 4.0 International license.[107] Copyright 2018, Nature Publishing Group.

### 4.3. Optical memory devices

Molecular electronics has gathered a great attention as a post-silicon technology for future nanoscale electronic devices.[193-195] The use of single molecules as memory elements can be attained by employing molecular switches featuring two independently stable states which can be accessed by means of an external stimulus, enabling to encode information as “0” and “1” in the same device. Among various molecular switches, photochromic molecules can undergo reversible photoisomerization between two or more states upon irradiation with light at different wavelengths. These states can exhibit markedly different characteristics including the electronic energy levels, electrical conductivity, or other photophysical properties. Thus, the photoswitchable properties of photochromic molecules provide tools to achieve electrically bistable states in the optically controlled memory device.

Diarylethenes combine key characteristics which are essential to realize memory devices such as large conductance changes, fast photo-isomerization, very high fatigue resistance, and thermodynamic stability of both open and closed isomers.[25, 196] Upon UV irradiation, the open form of diarylethene undergoes isomerization to the closed form yielding a completely π-conjugated core which can be used as a path to transfer charges through the molecule. In contrast, upon exposure of the closed form of diarylethene to visible light the open isomer is re-generated. In the latter, the absence of an extended conjugation breaks up the current path into two rather decoupled systems. From the perspective of the molecular energy levels

(Figure 3c), the closed form of diarylethene shows the higher HOMO energy level and the reduced band gap when compared to the open isomer.[149] The past research works showed that the great challenge of the diarylethene based memory device consists in retaining its molecular switching properties when sandwiched between solid-state electrodes due to the sensitivity of the molecules when coupled to the outer environment.[197] Therefore, in practice, two kinds of electrode materials have been employed by Kim *et al.* in the diarylethene-based memory devices, which are conducting polymer/Au bilayer electrode and rGO electrode, respectively.[109, 198] The device with the polymer/Au bilayer electrode did not show the optically switchable behavior, possibly because of the low optical transmission characteristics of the electrode bilayer and the strong coupling between the molecules and the electrodes.[198] In contrast, the device with rGO electrode preserved the switching behavior and showed excellent memory performance.[109] **Figure 8**a portrays the fabrication process and the final device structure. A monolayer of diarylethene molecules is sandwiched between a gold bottom electrode and a spray-coated rGO top electrode. The state of the diarylethenes can be defined and fixed by light irradiation during the device fabrication and operation. The retention time of the memory device is an important figure of merit for the practical applications. Therefore, the authors measured the current density of both the closed- and open-state device for up to $10^4$ s. Figure 8b shows no obvious degradation of the current density during the whole test for the two electrical states. After 30-days storage under ambient conditions, the device still preserves the defined electrical states without noticeable current change. The reversible photoswitching behavior is crucial for the application as optical memory device. Figure 8c displays the current-voltage curves of the device under different light stimuli. The initial high conductance state (closed form) is converted to the low conductance state (open form) upon visible light irradiation, and then converted back to the high conductance state (closed form again) after exposure to UV light. The authors have further performed alternating light irradiation by UV and visible light on the memory device

for 10 cycles to test the switching stability. Figure 8d provides evidence for a high fatigue resistance of the diarylethenes with a high reproducibility of the two electrical states. The device after 30-day storage also keeps the reliable and reversible photoswitching behavior. All these results demonstrate the importance of the rGO top electrodes for the realization of the optical memory device based on diarylethenes. Another representative work based on graphene/diarylethene hybrid system is a single-molecule junction, in which graphene and diarylethene operate as electrode and channel materials, respectively.[193] This covalently bonded junction shows light-controlled current switching with $I_{on}/I_{off}$ ratio ~100, over 1-year stability and over 100-cycle reproducibility.

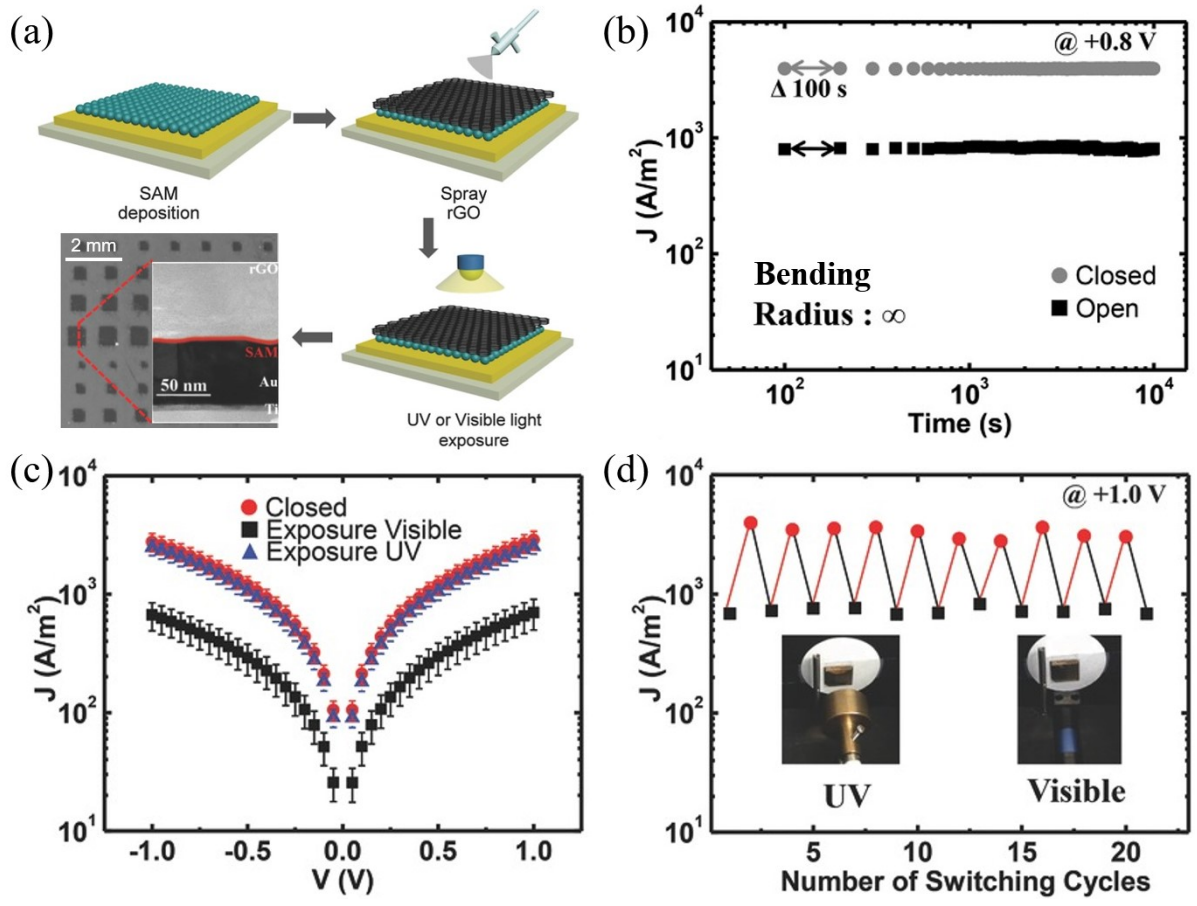


**Figure 8.** (a) Schematics illustrating the device fabrication processes. A monolayer of diarylethene molecules is first assembled on the Au bottom electrode and then the rGO was spray-coated onto the molecular surface as the top electrode. The final device is exposed to the UV or visible light working as optical memory. The cross-sectional TEM image of the device clearly shows the sandwiched structure. (b) Retention characteristics for the closed and open states of the device for up to $10^4$ s. (c) Current-voltage curves of the optical memory device at initial closed states, open states that were converted from the closed states with visible light exposure, and closed states that were converted back from the open states with

UV light exposure. (d) The reversible photoswitching characteristics repeated 20 times by alternating UV and visible light exposure. Adapted with permission.[109] Copyright 2015, Wiley-VCH.

Azobenzenes show a large conformational change during photoisomerization and sizable change in dipole moment. Based on its unique photophysical properties, such a photochromic molecule was also exploited as channel material for constructing optical memory devices. In contrast to diarylethene, the conductance, the molecular energy levels, and the bandgaps of the azobenzene isomers do not show significant changes. Therefore, it is crucial to find a physical property which enables to achieve bistable resistance states with large $I_{on}/I_{off}$ ratio in azobenzene-based devices. The idea consists in sandwiching azobenzene molecules between two electrodes and tune the tunneling current by reversibly switching the molecular length. Through the selection of the appropriate electrode materials and the design of the azobenzene molecules to optimize the interaction with the electrode layer, Seo *et al.* were able to develop photoswitchable devices with two relatively stable resistance states.[199] Large-area monolayer graphene grown by chemical vapor deposition (CVD) method worked as the bottom and top electrode. The molecules with diazonium moiety were covalently grafted onto the surface of the bottom graphene electrode. The other extremity of the molecules exposed the photochromic azobenzene unit, which was placed in physical contact with the graphene top electrode (**Figure 9**a). Before performing the characterization of the photochromic devices, the control experiment was carried out to estimate the molecular coverage and verify the electrical transport mechanism. Three phenyl-terminated alkanes with different length of the saturated chain have been sandwiched between the graphene electrodes. The degree of functionalization, as estimated by *in-situ* nanogravimetric tests, revealed the grafting of one molecule each nine $sp^2$ carbon atoms of graphene. The devices with shortest channel lengths (PhC8 in Figure 9b) exhibited the highest current density. The latter was found to decrease exponentially with the increasing molecular length, providing unambiguous evidence for a

tunneling mechanism ruling the transport through the junction. When adding the azobenzene functional head group at the extremity of the phenyl-terminated alkanes, the devices showed light-controlled electrical transport (Figure 9c). After UV light irradiation, the molecules were converted from *trans* to *cis* form and the current increased of one order of magnitude. Then the current decreases back to the previous value upon exposure to visible light (triggering the *cis* to *trans* back conversion). The photoswitching of the azobenzene molecules changed the vertical distance of the bottom and top electrodes. The decrease of molecular length in the *cis* form resulted in the lowering of the tunneling barrier and hence the increase of the device current. Over 50 cycles of alternating UV and visible light irradiation were performed to test the stability of the devices and the current density plot at 0.3 V voltage bias in Figure 9d displays almost identical and reproducible results at both molecular states, indicating the highly stable photoswitchable devices. The successful photoswitching of the current in azobenzene devices with high stability demonstrated the possibility to construct azobenzene-based optical memories.

Alongside the achievement of two resistance states, Margapoti *et al.* reported the observation of quasibound states of graphene by inserting azobenzenes SAM in-between graphene and Au electrodes.[200] The azobenzene derivative exposing a thiol anchoring group could be chemisorbed onto the Au bottom electrode and the mechanically exfoliated graphene layer was transferred onto the top of SAM to operate as top electrode. The device structure is similar to that shown in Figure 7a and the alkanethiol spacers are also sandwiched between the electrodes to prevent steric hindrance of the photo-mediated molecular conformation switching. The azobenzene molecules were vertically standing on the surface of gold and the molecular length could be switched between 1.90 nm (*trans* form) and 1.45 nm (*cis* form). The current-voltage curves of the device measured in a conductive AFM based junction revealed two resistance states with large $I_{on}/I_{off}$ ratio exceeding 100. Furthermore, the authors observed the pronounced current peaks with every 100 meV voltage gap in the device with

*cis*-AZO. This resonance oscillations of the current could be ascribed mainly to the local gating effect (change of molecular dipole moment) of the *cis* form on the nearby graphene layer. Through the change of the molecular conformation, it was possible to *in-situ* modify the scattering potential of the surrounding graphene layers. Hence, the photochromic molecules provided a convenient method to reversibly modulate the fundamental physical properties of graphene.

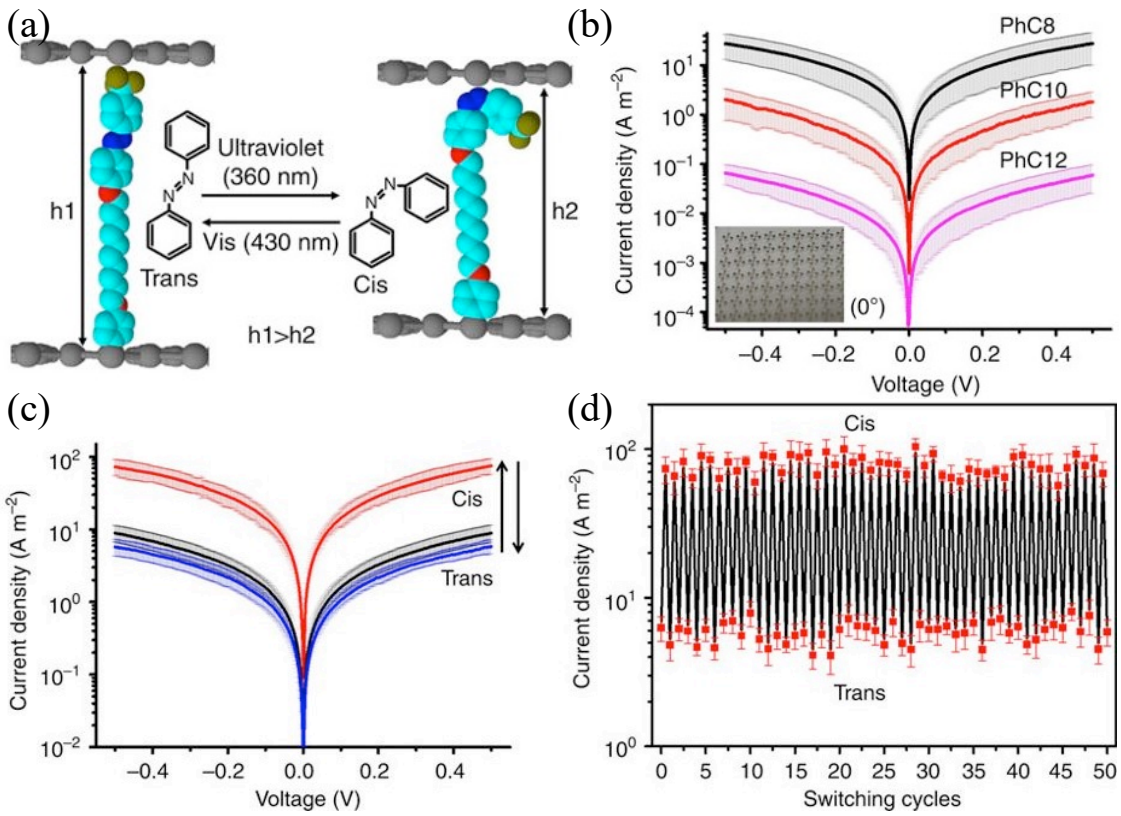


**Figure 9.** (a) The schematic of graphene-aryl azobenzene monolayer-graphene devices. The light irradiation can induce the conformational changes of the azobenzene molecules and modulate the molecular tunneling barriers. (b) Current density-voltage plots for the aryl alkane monolayer with different molecular lengths. (c) Current density-voltage plots of aryl azobenzene devices with photo-induced reversible switching. (d) The photo-induced current switching between two isomer states of aryl azobenzene devices for over 50 cycles. Adapted with permission.[199] Copyright 2013, Nature Publishing Group.

The azobenzene molecules can be switched not only by light, but also by means of an electric field. Min *et al.* replaced the graphene electrode in Figure 9a with rGO and fabricated the voltage-controlled molecular memory devices.[132] The applied positive and negative electric field between the electrodes could interconvert the molecules between the *trans* and *cis* states,

thereby modulating the conductance states in the memory devices. The devices exhibited good memory retention and write-read-erase-read performance. In another report, a pyrene functionalized azobenzene derivative was covalently bonded to the side chain of polymethylmethacrylate (PMMA) yielding a novel light-responsive AZO-PMMA copolymer.[166] The polar orientation of the azobenzene derivative could be controlled by the photo-assistant poling process and erased by photo-depoling process. Under positive (negative) poling voltage and light irradiation (λ=479 nm), the copolymer showed downward (upward) remnant polarization and acted as an external gate to switch the carrier density of the underlying graphene layer. The quasi-remnant polarization of copolymer induced the electrons/holes injection and the Fermi level change of graphene, setting the "+1"/"-1" states. Under the light irradiation without electrical field, the molecules recovered to random polarization (photo-depoling process) and the resistance states returned to the pristine state "0". The resistance change ratio of "+1"/"-1" states to "0" state could be as large as 60%. This novel optically-controlled device demonstrated a ternary-logic transistor with nonvolatile memory characteristics.

Recently Döbbelin *et al.* proposed a new methodology to construct the hybrid system with bistable conductance states.[201] During the liquid-phase exfoliation of graphite, alkyl-substituted azobenzenes were added as dispersion-stabilizing agents to improve the exfoliation efficiency. The graphene layers functionalized by photochromic molecules during the exfoliation process and the composites thereof could be used in the light-responsive electronic devices with controllable resistance states. Raman spectroscopy analysis of the composites revealed the co-existence of both the graphene and azobenzene peaks, indicating the successful functionalization. The intensity ratio of two azobenzene peaks at ~1417 $cm^{-1}$ and ~1442 $cm^{-1}$ was found being light-responsive, thus confirming the efficient photoisomerization in the composite. Such composites were drop-cast onto $SiO_2$/Si substrates exposing pre-patterned interdigitated gold electrodes forming a 100-nm-thick film. The

current measured while alternating UV and visible light irradiation cycles showed a lower current in the *cis* form and a higher current in the *trans* form. Azobenzene molecules were physisorbed flat on the top and in-between the graphene sheets due to the long alkyl chain. The switching from *trans* to *cis* form induced the increase of graphene interlayer distance and hindered the hopping transport of charge carriers between the sheets, hence resulting in the lower current.

The working mechanism and the memory performance of optically-switchable molecular devices with 2D electrodes is summarized in **Table 4**.

**Table 4.** Optically-switchable molecular device with 2D materials as metal electrode.

| Molecule | 2D material | Bond type | Working mechanism | $I_{on}/I_{off}$ ratio | Stability | Reproducibility | Ref. |
|---|---|---|---|---|---|---|---|
| DAE | rGO | Non-covalent | MC | <10 | 30 days | >10 cycles, retention $10^4$ s | [109] |
| AZO | Graphene | both | Tunneling | ~10 | | >50 cycles | [199] |
| AZO | Graphene | Non-covalent | Tunneling | <10 | | >6 cycles | [201] |
| DAE | Graphene | Covalent | | ~100 | >1 year | >100 cycles | [193] |

Note: DAE, diarylethene; rGO, reduced graphene oxide; MC, molecular conductivity change; AZO, azobenzene.

### 4.4. Capacitors

Graphene, with its ultrahigh relative surface area, is a promising material for capacitors, due to its high capability to store electrostatic charge.[202] Furthermore, the high conductivity of graphene sheets reduces the diffusion resistance, leading to enhanced power and energy density of capacitors. However, the processing of graphene thin films is hindered by the aggregation and restacking of graphene sheets due to π-π interaction and van der Waals forces among adjacent sheets.[203] This results in the decrease of surface areas and limitation in ions diffusion between graphene layers. Considerable research efforts have been addressed to tackle challenges such as adding spacer, template-assisted growth, and crumpling of the graphene sheets.[204-206] The most widely used spacers are carbonaceous material, metals or metal oxides, and other pseudocapacitive materials.[207-209] Chen *et al.* proposed a novel method by using photochromic azobenzene molecules as surfactant and spacer to

functionalize GO.[99] GO is a negatively charged material containing abundant carboxyl groups on basal planes and edges. Through electrostatic interactions, the cationic azobenzenes (structure shown in the top inset of **Figure 10**a and 10b) can be grafted on the surface of GO. The azobenzene-GO composites preserved the photoisomerization characteristics as confirmed by the UV-Vis absorption spectra. The absorption peak at 350 nm was found in the *trans*-azobenzene-GO composites due to the π–π* transition. The intensity of the absorption peak at 350 nm decreased after UV irradiation and recovered to the high level after exposure to blue light. The AFM images and the XRD patterns provided evidence for the ability of cationic azobenzene surfactants to change the morphology and aggregation of GO sheets. The *trans*-azobenzene has a lower polarity, which induced the hydrophobic nature of the surface thereby leading to a propensity of the composites to aggregate in the water, with the averaged 30 nm flake thickness. When azobenzene was converted into its *cis* form which features higher polarity, the sheets showed hydrophilic characteristics with an averaged 2 nm flake thickness. Such large aggregation change could effectively affect the capacitance of the GO sheets. Figure 10a and 10b show the electrochemical cyclic voltammograms (CV) of AZO-GO composites under different light irradiation. The UV light induced the increase of the specific capacitance of the composites from 51 F/g to 85 F/g. Then the capacitance decreased from 85 F/g to 63 F/g when exposure to blue light.[99] The bottom insets in Figure 10a and 10b schematically explain the change of the aggregation state in the composites with light irradiation. The photo-modulated aggregation states directly affected the surface area and the capacitance.

The supercapacitor is an energy storage device combining high capacitance, high power density, fast charge/discharge speed, and long cycle-life performance. The theoretical specific capacitance of monolayer graphene is as large as 550 F/g.[210] Therefore, graphene and graphene-related materials have been extensively explored as the electrode materials for supercapacitors.[211] The scaling down of the dimensions of electronic devices calls for the

development of miniaturized energy-storage components. Microsupercapacitors (MSC) with the advantages of supercapacitors and the minimized device dimensions are suitable for on-chip micropower energy sources. In addition, the controlled doping of graphene by molecules can modulate its capacitive behavior. Based on this concept, Liu *et al.* designed a photoswitchable MSC, composed of a diarylethene-graphene composite.[110] The diarylethene molecules (structure in Figure 10c) are physisorbed onto the graphene surface (grown by CVD method). Then, the Au current collector is deposited on the composites through a shadow mask, followed by oxygen plasma etching of the channels. Finally, the polymer gel electrolyte was drop-cast onto the interdigitated microelectrodes, thus yielding the all-solid-state MSC based on in-plane geometry (Figure 10c). Figure 10d shows the CV curves of the fabricated MSC and its light-responsive properties. The MSC can be operated at ultrahigh rates up to $10^4$ V/s, corresponding to the 0.2 ms charging-discharging time. The light-responsive CV curves showed that the total capacitance increases under UV irradiation, reaching 120% of its original value, while under white light irradiation, it decreased to the original value. The capacitance could be modulated for several cycles between high and low states with alternating UV and white light irradiation (Figure 10e). Such a capacitance change resulted from the joint effect of charge transfer between graphene and diarylethenes and the formation of interfacial dipoles. The light-controlled MSC opens up new opportunity for future portable and wearable multiresponsive power supplies.

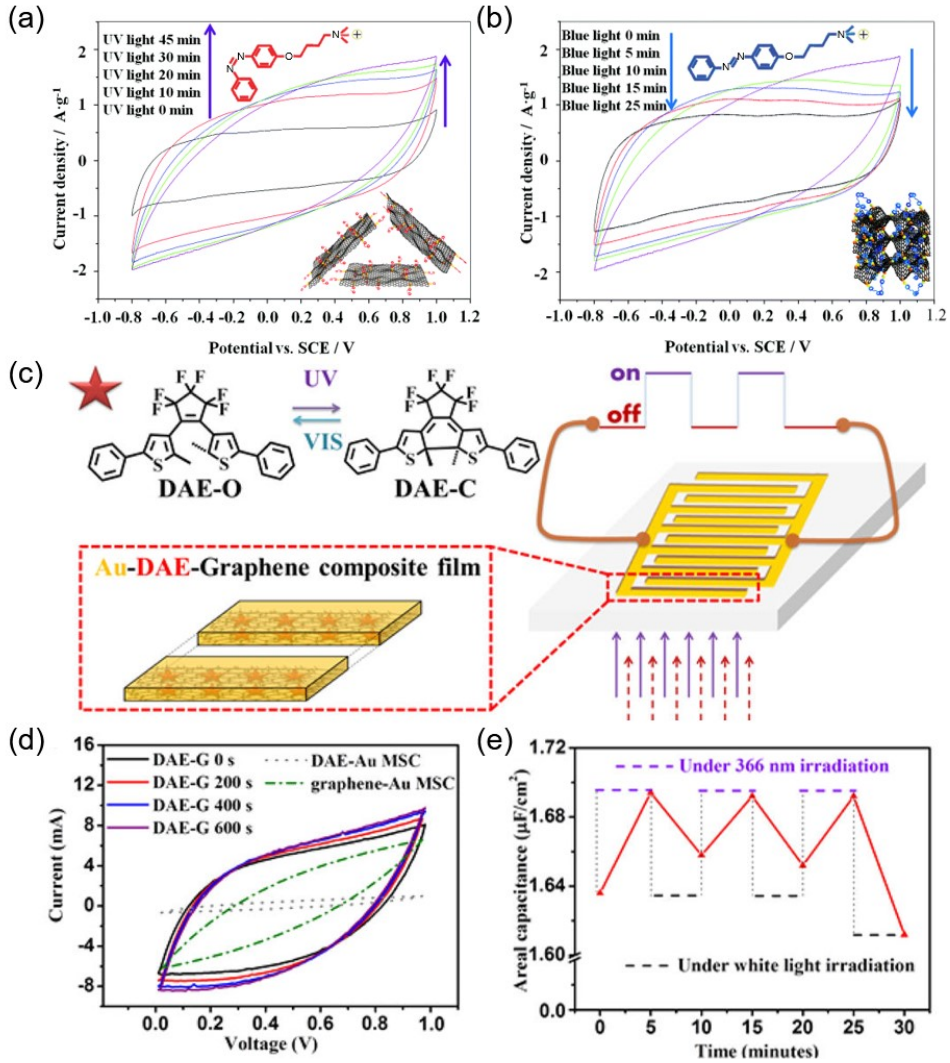


**Figure 10.** Cyclic voltammograms of (a) azobenzene-GO composites upton UV irradiation for different times, (b) UV light irradiated azobenzene-GO composites upon blue light irradiation for different times. Top inset shows the structure of the cationic azobenzene molecules. Bottom inset shows the schematic of the aggregation state of the composites. Adapted with permission.[99] Copyright 2015, Royal Society of Chemistry. (c) Schematic illustration of photoresponsive MSC device with diarylethene on the top of graphene electrodes. (d) CV curves of diarylethene-graphene MSC device after different UV irradiation times as well as MSC reference devices with diarylethene-Au or graphene-Au geometry. (e) The switching behavior of diarylethene-graphene MSC by alternating UV and white light irradiation. Adapted under an ACS AuthorChoice License.[110] Copyright 2017, American Chemical Society.

## 5. Conclusion

In this Progress Report, we have highlighted the most enlightening recent works on hybrid light-responsive systems based on the photosensitive molecules and 2D materials. We have summarized the switching mechanism of most representative photochromic molecules and the

unique optical properties of the photosensitive molecules. Through the covalent or non-covalent functionalization of 2D materials with photosensitive molecules, optically tunable properties of the hybrid 2D systems and the novel light-responsive devices for applications in electronic, optoelectronic and energy-related applications have been demonstrated with excellent performances which pave the way for further developments.

Despite the rapid progress in this field, numerous challenges need to be overcome to meet the requirements for practical applications. For the non-covalent functionalization, achieving an exquisite control over the process of molecular self-assembly on 2D surfaces, which requires *ad hoc* molecular design, is of paramount importance. The high degree of order can be regarded as a continuous and homogeneous molecules adlayer, which may reach the structural perfection of the superlattice, to maximizes the collective molecules/2D interaction. This hybrid van der Waals heterostructure constitutes a template for constructing hybrid materials with properties on demand and further used as the building block for novel devices. For the more robust covalent functionalization, the challenge is to minimize the degradation of the excellent properties of 2D layers. Ideally, molecules can serve not only as a mean to impart light-responsive properties to 2D materials, but also for simultaneously healing their structural (thus electronic) defects. The preferential bonding of molecules on the edge or the vacancy sites of 2D materials is a possible solution. The selection criterion among two types of functionalization methods depends on the device type and required performance, along with its structure and the thickness of 2D materials. For the 2D electronic devices with molecular doping, the non-covalent and covalent functionalization is commonly adopted on monolayer and few-layer 2D materials, respectively, in order to maximize the performance. In the molecular electronic devices with 2D electrodes, the covalent functionalization is mostly used to decrease the tunneling barrier. Another commonly encountered challenge in 2D optoelectronics is the persistent photoconductivity, which results in the long device photoresponse time and represents a major obstacle to efficiently operate light-responsive

devices. The possible solutions include the interface engineering for both the 2D/dielectric and 2D/molecule interface, and the improved 2D materials quality. Another interesting approach which could be exploited in the future in order to harness the light responsive nature of molecules-2D materials hybrids consists in the controlled coupling with the vacuum field as a means to modify their properties through the formation of hybrid light-matter states.[212] Overall, 2D materials are undoubtedly an ideal platform to construct high-performance light-responsive systems and devices by the functionalization of photosensitive molecules. These hybrid systems show potential for technological applications in multiple fields, ranging from photodetectors and biomedical imaging to optical-controllable logic, memory and energy-related devices. A variety of different combinations of 2D materials and photosensitive molecules merging the properties of both components should be explored thereby paving the way towards novel applications in future multi-responsive thus multifunctional optoelectronics.

**Acknowledgements**

We acknowledge funding from the European Commission through the Graphene Flagship Core 2 project (GA-785219), the Marie Sklodowska-Curie projects ITN project iSwitch (GA-642196) and the Marie-Curie IEF STELLAR (GA- 795615), the M-ERA.NET project MODIGLIANI, the Agence Nationale de la Recherche through the Labex projects CSC (ANR-10-LABX-0026 CSC) and NIE (ANR-11-LABX-0058 NIE) within the Investissement d'Avenir program (ANR-10-120 IDEX-0002-02), and the International Center for Frontier Research in Chemistry (icFRC).

Received: ((will be filled in by the editorial staff))
Revised: ((will be filled in by the editorial staff))
Published online: ((will be filled in by the editorial staff))

**References**

[1] K. S. Novoselov, A. K. Geim, S. V. Morozov, D. Jiang, Y. Zhang, S. V. Dubonos, I. V. Grigorieva, A. A. Firsov, *Science* **2004**, *306*, 666.
[2] A. C. Ferrari, F. Bonaccorso, V. Fal'ko, K. S. Novoselov, S. Roche, P. Bøggild, S. Borini, F. H. L. Koppens, V. Palermo, N. Pugno, J. A. Garrido, R. Sordan, A. Bianco, L. Ballerini, M. Prato, E. Lidorikis, J. Kivioja, C. Marinelli, T. Ryhänen, A. Morpurgo, J. N. Coleman, V. Nicolosi, L. Colombo, A. Fert, M. Garcia-Hernandez, A. Bachtold, G. F. Schneider, F. Guinea, C. Dekker, M. Barbone, Z. Sun, C. Galiotis, A. N. Grigorenko, G. Konstantatos, A. Kis, M. Katsnelson, L. Vandersypen, A. Loiseau, V. Morandi, D. Neumaier, E. Treossi, V. Pellegrini, M. Polini, A. Tredicucci, G. M. Williams, B. Hee Hong, J.-H. Ahn, J. Min Kim, H. Zirath, B. J. van Wees, H. van der Zant, L. Occhipinti, A. Di Matteo, I. A. Kinloch, T. Seyller, E. Quesnel, X. Feng, K. Teo, N. Rupesinghe, P. Hakonen, S. R. T. Neil, Q. Tannock, T. Löfwander, J. Kinaret, *Nanoscale* **2015**, *7*, 4598.
[3] K. F. Mak, C. Lee, J. Hone, J. Shan, T. F. Heinz, *Phys. Rev. Lett.* **2010**, *105*, 136805.
[4] F. Wang, Y. Zhang, C. Tian, C. Girit, A. Zettl, M. Crommie, Y. R. Shen, *Science* **2008**, *320*, 206.
[5] W. Jie, Z. Yang, G. Bai, J. Hao, *Advanced Optical Materials* **2018**, *6*, 1701296.
[6] Q. H. Wang, K. Kalantar-Zadeh, A. Kis, J. N. Coleman, M. S. Strano, *Nat. Nanotechnol.* **2012**, *7*, 699.
[7] F. Bonaccorso, Z. Sun, T. Hasan, A. C. Ferrari, *Nat. Photonics* **2010**, *4*, 611.
[8] K. F. Mak, J. Shan, *Nat. Photonics* **2016**, *10*, 216.
[9] G. Fiori, F. Bonaccorso, G. Iannaccone, T. Palacios, D. Neumaier, A. Seabaugh, S. K. Banerjee, L. Colombo, *Nat. Nanotechnol.* **2014**, *9*, 768.
[10] X. Huang, Z. Zeng, Z. Fan, J. Liu, H. Zhang, *Adv. Mater.* **2012**, *24*, 5979.
[11] D. Jariwala, V. K. Sangwan, L. J. Lauhon, T. J. Marks, M. C. Hersam, *ACS Nano* **2014**, *8*, 1102.
[12] X. Duan, C. Wang, A. Pan, R. Yu, X. Duan, *Chem. Soc. Rev.* **2015**, *44*, 8859.
[13] R. Frisenda, A. J. Molina-Mendoza, T. Mueller, A. Castellanos-Gomez, H. S. J. van der Zant, *Chem. Soc. Rev.* **2018**, *47*, 3339.
[14] C. Anichini, W. Czepa, D. Pakulski, A. Aliprandi, A. Ciesielski, P. Samorì, *Chem. Soc. Rev.* **2018**, *47*, 4860.
[15] S. Bertolazzi, M. Gobbi, Y. Zhao, C. Backes, P. Samorì, *Chem. Soc. Rev.* **2018**, *47*, 6845.
[16] H. Schmidt, F. Giustiniano, G. Eda, *Chem. Soc. Rev.* **2015**, *44*, 7715.
[17] Y. Zhao, K. Xu, F. Pan, C. Zhou, F. Zhou, Y. Chai, *Adv. Funct. Mater.* **2017**, *27*, 1603484.
[18] S. Mura, J. Nicolas, P. Couvreur, *Nat. Mater.* **2013**, *12*, 991.
[19] M. A. C. Stuart, W. T. S. Huck, J. Genzer, M. Müller, C. Ober, M. Stamm, G. B. Sukhorukov, I. Szleifer, V. V. Tsukruk, M. Urban, F. Winnik, S. Zauscher, I. Luzinov, S. Minko, *Nat. Mater.* **2010**, *9*, 101.
[20] J. Cui, A. Del Campo, in *Smart Polymers and their Applications*, (Eds: M. R. Aguilar, J. San Román), Woodhead Publishing, **2014**, 93.
[21] P. Ceroni, A. Credi, M. Venturi, V. Balzani, *Photochem. Photobiol. Sci.* **2010**, *9*, 1561.
[22] C. Brieke, F. Rohrbach, A. Gottschalk, G. Mayer, A. Heckel, *Angew. Chem., Int. Ed.* **2012**, *51*, 8446.
[23] M.-M. Russew, S. Hecht, *Adv. Mater.* **2010**, *22*, 3348.
[24] K. Szaciłowski, *Chem. Rev.* **2008**, *108*, 3481.
[25] M. Irie, T. Fukaminato, K. Matsuda, S. Kobatake, *Chem. Rev.* **2014**, *114*, 12174.
[26] A. M. Kolpak, J. C. Grossman, *Nano Lett.* **2011**, *11*, 3156.

[27] Y. Huang, W. Zheng, Y. Qiu, P. Hu, *ACS Appl. Mater. Interfaces* **2016**, *8*, 23362.
[28] X. Liu, J. Gu, K. Ding, D. Fan, X. Hu, Y.-W. Tseng, Y.-H. Lee, V. Menon, S. R. Forrest, *Nano Lett.* **2017**, *17*, 3176.
[29] E. Orgiu, P. Samorì, *Adv. Mater.* **2014**, *26*, 1827.
[30] N. Li, H.-L. Jiang, X. Wang, X. Wang, G. Xu, B. Zhang, L. Wang, R.-S. Zhao, J.-M. Lin, *Trends Anal. Chem.* **2018**, *102*, 60.
[31] S. Cinti, F. Arduini, *Biosens. Bioelectron.* **2017**, *89*, 107.
[32] G. S. Hartley, *Nature* **1937**, *140*, 281.
[33] G. S. Hartley, *J. Chem. Soc.* **1938**, 633.
[34] E. V. Brown, G. R. Granneman, *J. Am. Chem. Soc.* **1975**, *97*, 621.
[35] E. Merino, M. Ribagorda, *Beilstein J. Org. Chem.* **2012**, *8*, 1071.
[36] H. Dürr, H. Bouas-Laurent, *Photochromism: molecules and systems*, Elsevier, 2003.
[37] E. H. Baker, F. C. Tompkins, H. A. Fahim, A. M. Fleifel, F. Bergmann, A. Kalmus, E. Fischer, Y. Hirshberg, H. R. V. Arnstein, E. R. Ward, L. A. Day, R. S. Bradley, W. Tadros, M. Kamel, A. S. Bailey, D. H. Bates, H. R. Ing, M. A. Warne, E. Neale, L. T. D. Williams, H. B. Henbest, A. G. Sharpe, A. H. Lamberton, E. P. Hart, C. A. Bunton, E. A. Halevi, J. P. Thurston, J. Walker, R. A. Robinson, F. G. Mann, B. B. Smith, D. L. Hammick, A. M. Roe, S. Peat, W. J. Whelan, G. J. Thomas, *J. Chem. Soc.* **1952**, 4518.
[38] L. Kortekaas, J. Chen, D. Jacquemin, W. R. Browne, *J. Phys. Chem. B* **2018**, *122*, 6423.
[39] R. Klajn, *Chem. Soc. Rev.* **2014**, *43*, 148.
[40] F. M. Raymo, *Adv. Mater.* **2002**, *14*, 401.
[41] F. M. Raymo, S. Giordani, *J. Am. Chem. Soc.* **2001**, *123*, 4651.
[42] M. Levitus, G. Glasser, D. Neher, P. F. Aramendía, *Chem. Phys. Lett.* **1997**, *277*, 118.
[43] M. Bletz, U. Pfeifer-Fukumura, U. Kolb, W. Baumann, *J. Phys. Chem. A* **2002**, *106*, 2232.
[44] M. Irie, M. Mohri, *J. Org. Chem.* **1988**, *53*, 803.
[45] M. Irie, *Chem. Rev.* **2000**, *100*, 1685.
[46] G. Reecht, C. Lotze, D. Sysoiev, T. Huhn, K. J. Franke, *ACS Nano* **2016**, *10*, 10555.
[47] E. Orgiu, N. Crivillers, M. Herder, L. Grubert, M. Pätzel, J. Frisch, E. Pavlica, D. T. Duong, G. Bratina, A. Salleo, N. Koch, S. Hecht, P. Samorì, *Nat. Chem.* **2012**, *4*, 675.
[48] J. Daub, T. Knöchel, A. Mannschreck, *Angew. Chem. Int. Ed. Engl.* **1984**, *23*, 960.
[49] H. Goerner, C. Fischer, S. Gierisch, J. Daub, *J. Phys. Chem.* **1993**, *97*, 4110.
[50] J. Ern, M. Petermann, T. Mrozek, J. Daub, K. Kuldová, C. Kryschi, *Chem. Phys.* **2000**, *259*, 331.
[51] L. Striepe, T. Baumgartner, *Chem. Eur. J.* **2017**, *23*, 16924.
[52] W. H. Perkin, *J. Chem. Soc.* **1868**, *21*, 53.
[53] B. N. Mattoo, *Trans. Faraday Soc.* **1956**, *52*, 1184.
[54] J. Donovalová, M. Cigáň, H. Stankovičová, J. Gašpar, M. Danko, A. Gáplovský, P. Hrdlovič, *Molecules* **2012**, *17*, 3259.
[55] Y.-F. Sun, S.-H. Xu, R.-T. Wu, Z.-Y. Wang, Z.-B. Zheng, J.-K. Li, Y.-P. Cui, *Dyes Pigm.* **2010**, *87*, 109.
[56] P. Rothemund, *J. Am. Chem. Soc.* **1935**, *57*, 2010.
[57] M. Gouterman, *J. Mol. Spectrosc.* **1961**, *6*, 138.
[58] M. Gouterman, *J. Chem. Phys* **1959**, *30*, 1139.
[59] R. Giovannetti, in *Macro To Nano Spectroscopy*, (Ed: J. Uddin), InTech, **2012**.
[60] J. Karolczak, D. Kowalska, A. Lukaszewicz, A. Maciejewski, R. P. Steer, *J. Phys. Chem. A* **2004**, *108*, 4570.
[61] R. P. Linstead, *J. Chem. Soc.* **1934**, 1016.
[62] Y. Rio, M. S. Rodríguez-Morgade, T. Torres, *Org. Biomol. Chem.* **2008**, *6*, 1877.
[63] K. Sakamoto, E. Ohno-Okumura, *Materials* **2009**, *2*, 1127.

[64] M. G. Walter, A. B. Rudine, C. C. Wamser, *J. Porphyrins Phthalocyanines* **2010**, *14*, 759.
[65] S. Luo, E. Zhang, Y. Su, T. Cheng, C. Shi, *Biomaterials* **2011**, *32*, 7127.
[66] D. Wróbel, A. Dudkowiak, *Mol. Cryst. Liq. Cryst.* **2006**, *448*, 15/[617].
[67] A. S. Polo, M. K. Itokazu, N. Y. Murakami Iha, *Coord. Chem. Rev.* **2004**, *248*, 1343.
[68] Q. Zhao, C. Huang, F. Li, *Chem. Soc. Rev.* **2011**, *40*, 2508.
[69] A. A. Martí, *J. Photochem. Photobiol. A Chem.* **2015**, *307-308*, 35.
[70] A. Vlček, S. Záliš, *Coord. Chem. Rev.* **2007**, *251*, 258.
[71] A. Loudet, K. Burgess, *Chem. Rev.* **2007**, *107*, 4891.
[72] T. Kowada, H. Maeda, K. Kikuchi, *Chem. Soc. Rev.* **2015**, *44*, 4953.
[73] C. S. Kue, S. Y. Ng, S. H. Voon, A. Kamkaew, L. Y. Chung, L. V. Kiew, H. B. Lee, *Photochem. Photobiol. Sci.* **2018**, *17*, 1691.
[74] W. Herbst, K. Hunger, G. Wilker, H. Ohleier, R. Winter, in *Industrial Organic Pigments*, Wiley-VCH, Weinheim, Germany **2005**, Ch. 3.
[75] T. Weil, T. Vosch, J. Hofkens, K. Peneva, K. Müllen, *Angew. Chem., Int. Ed.* **2010**, *49*, 9068.
[76] C. Huang, S. Barlow, S. R. Marder, *J. Org. Chem.* **2011**, *76*, 2386.
[77] M. Sadrai, L. Hadel, R. R. Sauers, S. Husain, K. Krogh-Jespersen, J. D. Westbrook, G. R. Bird, *J. Phys. Chem.* **1992**, *96*, 7988.
[78] F. Würthner, *Chem. Commun.* **2004**, 1564.
[79] X. Zhan, A. Facchetti, S. Barlow, T. J. Marks, M. A. Ratner, M. R. Wasielewski, S. R. Marder, *Adv. Mater.* **2011**, *23*, 268.
[80] J. E. Anthony, A. Facchetti, M. Heeney, S. R. Marder, X. Zhan, *Adv. Mater.* **2010**, *22*, 3876.
[81] M. Supur, Y. Kawashima, K. Mase, K. Ohkubo, T. Hasobe, S. Fukuzumi, *J. Phys. Chem. C* **2015**, *119*, 13488.
[82] J. Balapanuru, G. Chiu, C. Su, N. Zhou, Z. Hai, Q.-h. Xu, K. P. Loh, *ACS Appl. Mater. Interfaces* **2015**, *7*, 880.
[83] S. Wieghold, J. Li, P. Simon, M. Krause, Y. Avlasevich, C. Li, J. A. Garrido, U. Heiz, P. Samorì, K. Müllen, F. Esch, J. V. Barth, C.-A. Palma, *Nat. Commun.* **2016**, *7*, 10700.
[84] L. Dubinsky, B. P. Krom, M. M. Meijler, *Bioorg. Med. Chem.* **2012**, *20*, 554.
[85] M. Gobbi, S. Bonacchi, J. X. Lian, Y. Liu, X.-Y. Wang, M.-A. Stoeckel, M. A. Squillaci, G. D'Avino, A. Narita, K. Müllen, X. Feng, Y. Olivier, D. Beljonne, P. Samorì, E. Orgiu, *Nat. Commun.* **2017**, *8*, 14767.
[86] V. Georgakilas, J. N. Tiwari, K. C. Kemp, J. A. Perman, A. B. Bourlinos, K. S. Kim, R. Zboril, *Chem. Rev.* **2016**, *116*, 5464.
[87] K. S. Mali, J. Greenwood, J. Adisoejoso, R. Phillipson, S. De Feyter, *Nanoscale* **2015**, *7*, 1566.
[88] W. Feng, W. Luo, Y. Feng, *Nanoscale* **2012**, *4*, 6118.
[89] B. Rybtchinski, *ACS Nano* **2011**, *5*, 6791.
[90] X. Zhuang, Y. Mai, D. Wu, F. Zhang, X. Feng, *Adv. Mater.* **2015**, *27*, 403.
[91] A. Ciesielski, P. Samorì, *Adv. Mater.* **2016**, *28*, 6030.
[92] J. P. Rabe, S. Buchholz, *Science* **1991**, *253*, 424.
[93] S. Cincotti, J. P. Rabe, *Appl. Phys. Lett.* **1993**, *62*, 3531.
[94] R. J. Chen, Y. Zhang, D. Wang, H. Dai, *J. Am. Chem. Soc.* **2001**, *123*, 3838.
[95] D. M. Guldi, G. M. A. Rahman, N. Jux, D. Balbinot, U. Hartnagel, N. Tagmatarchis, M. Prato, *J. Am. Chem. Soc.* **2005**, *127*, 9830.
[96] C. Backes, F. Hauke, A. Hirsch, *Adv. Mater.* **2011**, *23*, 2588.
[97] Y. Song, J. He, C. Peng, D. Hu, E. Ou, Y. Li, H. Peng, L. Bao, C. Shu, T. Gao, W. Xu, *Chem. Lett.* **2014**, *43*, 868.
[98] R. S. Swathi, K. L. Sebastian, *J. Chem. Phys* **2008**, *129*, 054703.

[99] S. Chen, L. Bao, E. Ou, C. Peng, W. Wang, W. Xu, *Nanoscale* **2015**, *7*, 19673.
[100] Y. Li, Y. Duan, J. Zheng, J. Li, W. Zhao, S. Yang, R. Yang, *Anal. Chem.* **2013**, *85*, 11456.
[101] A. R. Jang, E. K. Jeon, D. Kang, G. Kim, B.-S. Kim, D. J. Kang, H. S. Shin, *ACS Nano* **2012**, *6*, 9207.
[102] Q. Zhao, Y. Zhou, Y. Li, W. Gu, Q. Zhang, J. Liu, *Anal. Chem.* **2016**, *88*, 1892.
[103] S. Le Liepvre, P. Du, D. Kreher, F. Mathevet, A.-J. Attias, C. Fiorini-Debuisschert, L. Douillard, F. Charra, *ACS Photonics* **2016**, *3*, 2291.
[104] M. Supur, K. Ohkubo, S. Fukuzumi, *Chem. Commun.* **2014**, *50*, 13359.
[105] C. Wang, S. Yang, M. Yi, C. Liu, Y. Wang, J. Li, Y. Li, R. Yang, *ACS Appl. Mater. Interfaces* **2014**, *6*, 9768.
[106] A. Liscio, K. Kouroupis-Agalou, A. Kovtun, E. Gebremedhn, M. El Garah, W. Rekab, E. Orgiu, L. Giorgini, P. Samorì, D. Beljonne, V. Palermo, *ChemPlusChem* **2017**, *82*, 358.
[107] M. Gobbi, S. Bonacchi, J. X. Lian, A. Vercouter, S. Bertolazzi, B. Zyska, M. Timpel, R. Tatti, Y. Olivier, S. Hecht, M. V. Nardi, D. Beljonne, E. Orgiu, P. Samorì, *Nat. Commun.* **2018**, *9*, 2661.
[108] J. Li, J. Wierzbowski, Ö. Ceylan, J. Klein, F. Nisic, T. L. Anh, F. Meggendorfer, C.-A. Palma, C. Dragonetti, J. V. Barth, J. J. Finley, E. Margapoti, *Appl. Phys. Lett.* **2014**, *105*, 241116.
[109] D. Kim, H. Jeong, W.-T. Hwang, Y. Jang, D. Sysoiev, E. Scheer, T. Huhn, M. Min, H. Lee, T. Lee, *Adv. Funct. Mater.* **2015**, *25*, 5918.
[110] Z. Liu, H. I. Wang, A. Narita, Q. Chen, Z. Mics, D. Turchinovich, M. Kläui, M. Bonn, K. Müllen, *J. Am. Chem. Soc.* **2017**, *139*, 9443.
[111] X. Yu, A. Rahmanudin, X. A. Jeanbourquin, D. Tsokkou, N. Guijarro, N. Banerji, K. Sivula, *ACS Energy Lett.* **2017**, *2*, 524.
[112] C. Wang, D. Niu, B. Liu, S. Wang, X. Wei, Y. Liu, H. Xie, Y. Gao, *J. Phys. Chem. C* **2017**, *121*, 18084.
[113] H. Zhang, J. Ji, A. A. Gonzalez, J. H. Choi, *J. Mater. Chem. C* **2017**, *5*, 11233.
[114] Y. Huang, F. Zhuge, J. Hou, L. Lv, P. Luo, N. Zhou, L. Gan, T. Zhai, *ACS Nano* **2018**.
[115] A. Banerjee, B. Kundu, A. J. Pal, *Phys. Chem. Chem. Phys.* **2017**, *19*, 28450.
[116] J. H. Park, A. Sanne, Y. Guo, M. Amani, K. Zhang, H. C. P. Movva, J. A. Robinson, A. Javey, J. Robertson, S. K. Banerjee, A. C. Kummel, *Sci. Adv.* **2017**, *3*.
[117] T. R. Kafle, B. Kattel, S. D. Lane, T. Wang, H. Zhao, W.-L. Chan, *ACS Nano* **2017**, *11*, 10184.
[118] C. Wang, D. Niu, H. Xie, B. Liu, S. Wang, M. Zhu, Y. Gao, *J. Chem. Phys* **2017**, *147*, 064702.
[119] P. Huang, H. Zhu, L. Jing, Y. Zhao, X. Gao, *ACS Nano* **2011**, *5*, 7945.
[120] V. B. Engelkes, J. M. Beebe, C. D. Frisbie, *J. Am. Chem. Soc.* **2004**, *126*, 14287.
[121] X. Zhang, L. Hou, P. Samorì, *Nat. Commun.* **2016**, *7*, 11118.
[122] X. Zhang, Y. Feng, P. Lv, Y. Shen, W. Feng, *Langmuir* **2010**, *26*, 18508.
[123] P. Nguyen, J. Li, T. S. Sreeprasad, K. Jasuja, N. Mohanty, M. Ikenberry, K. Hohn, V. B. Shenoy, V. Berry, *Small* **2013**, *9*, 3823.
[124] S. M. Sharker, C. J. Jeong, S. M. Kim, J.-E. Lee, J. H. Jeong, I. In, H. Lee, S. Y. Park, *Chem. Asian J.* **2014**, *9*, 2921.
[125] A.-A. Nahain, J.-E. Lee, J. H. Jeong, S. Y. Park, *Biomacromolecules* **2013**, *14*, 4082.
[126] M. Maggini, G. Scorrano, M. Prato, *J. Am. Chem. Soc.* **1993**, *115*, 9798.
[127] D. Tasis, N. Tagmatarchis, A. Bianco, M. Prato, *Chem. Rev.* **2006**, *106*, 1105.
[128] M. Quintana, K. Spyrou, M. Grzelczak, W. R. Browne, P. Rudolf, M. Prato, *ACS Nano* **2010**, *4*, 3527.
[129] J. H. Lee, J. Jaworski, J. H. Jung, *Nanoscale* **2013**, *5*, 8533.

[130] Y. Feng, H. Liu, W. Luo, E. Liu, N. Zhao, K. Yoshino, W. Feng, *Sci. Rep.* **2013**, *3*, 3260.
[131] W. Luo, Y. Feng, C. Qin, M. Li, S. Li, C. Cao, P. Long, E. Liu, W. Hu, K. Yoshino, W. Feng, *Nanoscale* **2015**, *7*, 16214.
[132] M. Min, S. Seo, S. M. Lee, H. Lee, *Adv. Mater.* **2013**, *25*, 7045.
[133] J. Lu, A. Lipatov, N. S. Vorobeva, D. S. Muratov, A. Sinitskii, *Adv. Electron. Mater.* **2018**, *4*, 1800021.
[134] D. Wang, G. Ye, X. Wang, X. Wang, *Adv. Mater.* **2011**, *23*, 1122.
[135] J. L. Bahr, J. M. Tour, *Chem. Mater.* **2001**, *13*, 3823.
[136] C. A. Dyke, J. M. Tour, *J. Am. Chem. Soc.* **2003**, *125*, 1156.
[137] H.-X. Wang, K.-G. Zhou, Y.-L. Xie, J. Zeng, N.-N. Chai, J. Li, H.-L. Zhang, *Chem. Commun.* **2011**, *47*, 5747.
[138] H. Yan, L. Zhu, X. Li, A. Kwok, X. Pan, Y. Zhao, *Asian J. Org. Chem.* **2012**, *1*, 314.
[139] S. G. McAdams, E. A. Lewis, J. R. Brent, S. J. Haigh, A. G. Thomas, P. O'Brien, F. Tuna, D. J. Lewis, *Adv. Funct. Mater.* **2017**, *27*, 1703646.
[140] A. Tuxen, J. Kibsgaard, H. Gøbel, E. Lægsgaard, H. Topsøe, J. V. Lauritsen, F. Besenbacher, *ACS Nano* **2010**, *4*, 4677.
[141] K. C. Knirsch, N. C. Berner, H. C. Nerl, C. S. Cucinotta, Z. Gholamvand, N. McEvoy, Z. Wang, I. Abramovic, P. Vecera, M. Halik, S. Sanvito, G. S. Duesberg, V. Nicolosi, F. Hauke, A. Hirsch, J. N. Coleman, C. Backes, *ACS Nano* **2015**, *9*, 6018.
[142] D. Voiry, A. Goswami, R. Kappera, C. d. C. C. e. Silva, D. Kaplan, T. Fujita, M. Chen, T. Asefa, M. Chhowalla, *Nat. Chem.* **2015**, *7*, 45.
[143] G. Tuci, D. Mosconi, A. Rossin, L. Luconi, S. Agnoli, M. Righetto, C. Pham-Huu, H. Ba, S. Cicchi, G. Granozzi, G. Giambastiani, *Chem. Mater.* **2018**, *30*, 8257.
[144] X. Chen, D. McAteer, C. McGuinness, I. Godwin, J. N. Coleman, A. R. McDonald, *Chem. Eur. J.* **2018**, *24*, 351.
[145] A. Splendiani, L. Sun, Y. Zhang, T. Li, J. Kim, C.-Y. Chim, G. Galli, F. Wang, *Nano Lett.* **2010**, *10*, 1271.
[146] W. Zhao, Z. Ghorannevis, L. Chu, M. Toh, C. Kloc, P.-H. Tan, G. Eda, *ACS Nano* **2013**, *7*, 791.
[147] D. Xiao, G.-B. Liu, W. Feng, X. Xu, W. Yao, *Phys. Rev. Lett.* **2012**, *108*, 196802.
[148] J. M. Simmons, I. In, V. E. Campbell, T. J. Mark, F. Léonard, P. Gopalan, M. A. Eriksson, *Phys. Rev. Lett.* **2007**, *98*, 086802.
[149] M. Herder, F. Eisenreich, A. Bonasera, A. Grafl, L. Grubert, M. Pätzel, J. Schwarz, S. Hecht, *Chem. Eur. J.* **2017**, *23*, 3743.
[150] Y. L. Huang, Y. J. Zheng, Z. Song, D. Chi, A. T. S. Wee, S. Y. Quek, *Chem. Soc. Rev.* **2018**, *47*, 3241.
[151] K. F. Mak, K. He, C. Lee, G. H. Lee, J. Hone, T. F. Heinz, J. Shan, *Nat. Mater.* **2012**, *12*, 207.
[152] Z. Y. Zhu, Y. C. Cheng, U. Schwingenschlögl, *Phys. Rev. B* **2011**, *84*, 153402.
[153] Y. Lin, X. Ling, L. Yu, S. Huang, A. L. Hsu, Y.-H. Lee, J. Kong, M. S. Dresselhaus, T. Palacios, *Nano Lett.* **2014**, *14*, 5569.
[154] F. H. L. Koppens, T. Mueller, P. Avouris, A. C. Ferrari, M. S. Vitiello, M. Polini, *Nat. Nanotechnol.* **2014**, *9*, 780.
[155] R. R. Nair, P. Blake, A. N. Grigorenko, K. S. Novoselov, T. J. Booth, T. Stauber, N. M. R. Peres, A. K. Geim, *Science* **2008**, *320*, 1308.
[156] A. B. Kuzmenko, E. van Heumen, F. Carbone, D. van der Marel, *Phys. Rev. Lett.* **2008**, *100*, 117401.
[157] F. Yan, Z. Wei, X. Wei, Q. Lv, W. Zhu, K. Wang, *Small Methods* **2018**, *2*, 1700349.
[158] M. Long, P. Wang, H. Fang, W. Hu, *Adv. Funct. Mater.* **2019**, 1803807. DOI:10.1002/adfm.201803807.

[159] S. H. Yu, Y. Lee, S. K. Jang, J. Kang, J. Jeon, C. Lee, J. Y. Lee, H. Kim, E. Hwang, S. Lee, J. H. Cho, *ACS Nano* **2014**, *8*, 8285.
[160] Y. Yong, L. Zhou, Z. Gu, L. Yan, G. Tian, X. Zheng, X. Liu, X. Zhang, J. Shi, W. Cong, W. Yin, Y. Zhao, *Nanoscale* **2014**, *6*, 10394.
[161] H. Liu, A. T. Neal, P. D. Ye, *ACS Nano* **2012**, *6*, 8563.
[162] B. Radisavljevic, A. Radenovic, J. Brivio, V. Giacometti, A. Kis, *Nat. Nanotechnol.* **2011**, *6*, 147.
[163] O. Lopez-Sanchez, D. Lembke, M. Kayci, A. Radenovic, A. Kis, *Nat. Nanotechnol.* **2013**, *8*, 497.
[164] S. B. Desai, S. R. Madhvapathy, A. B. Sachid, J. P. Llinas, Q. Wang, G. H. Ahn, G. Pitner, M. J. Kim, J. Bokor, C. Hu, H.-S. P. Wong, A. Javey, *Science* **2016**, *354*, 99.
[165] M. Kim, N. S. Safron, C. Huang, M. S. Arnold, P. Gopalan, *Nano Lett.* **2012**, *12*, 182.
[166] C.-Y. Lin, C.-S. Chang, J. H. Lin, C.-C. Hsu, F. S.-S. Chien, *Appl. Phys. Lett.* **2013**, *102*, 013505.
[167] N. Peimyoo, J. Li, J. Shang, X. Shen, C. Qiu, L. Xie, W. Huang, T. Yu, *ACS Nano* **2012**, *6*, 8878.
[168] P. Joo, B. J. Kim, E. K. Jeon, J. H. Cho, B.-S. Kim, *Chem. Commun.* **2012**, *48*, 10978.
[169] S.-L. Li, K. Tsukagoshi, E. Orgiu, P. Samorì, *Chem. Soc. Rev.* **2016**, *45*, 118.
[170] T. Roy, M. Tosun, J. S. Kang, A. B. Sachid, S. B. Desai, M. Hettick, C. C. Hu, A. Javey, *ACS Nano* **2014**, *8*, 6259.
[171] I. Meric, M. Y. Han, A. F. Young, B. Ozyilmaz, P. Kim, K. L. Shepard, *Nat. Nanotechnol.* **2008**, *3*, 654.
[172] B. Li, A. V. Klekachev, M. Cantoro, C. Huyghebaert, A. Stesmans, I. Asselberghs, S. De Gendt, S. De Feyter, *Nanoscale* **2013**, *5*, 9640.
[173] X. Cui, G.-H. Lee, Y. D. Kim, G. Arefe, P. Y. Huang, C.-H. Lee, D. A. Chenet, X. Zhang, L. Wang, F. Ye, F. Pizzocchero, B. S. Jessen, K. Watanabe, T. Taniguchi, D. A. Muller, T. Low, P. Kim, J. Hone, *Nat. Nanotechnol.* **2015**, *10*, 534.
[174] Z. Yu, Y. Pan, Y. Shen, Z. Wang, Z.-Y. Ong, T. Xu, R. Xin, L. Pan, B. Wang, L. Sun, J. Wang, G. Zhang, Y. W. Zhang, Y. Shi, X. Wang, *Nat. Commun.* **2014**, *5*, 5290.
[175] Y. Zhao, J. Qiao, Z. Yu, P. Yu, K. Xu, P. Lau Shu, W. Zhou, Z. Liu, X. Wang, W. Ji, Y. Chai, *Adv. Mater.* **2017**, *29*, 1604230.
[176] Y. Zhao, J. Qiao, P. Yu, Z. Hu, Z. Lin, S. P. Lau, Z. Liu, W. Ji, Y. Chai, *Adv. Mater.* **2016**, *28*, 2399.
[177] A. C. Ferrari, D. M. Basko, *Nat. Nanotechnol.* **2013**, *8*, 235.
[178] A. Das, S. Pisana, B. Chakraborty, S. Piscanec, S. K. Saha, U. V. Waghmare, K. S. Novoselov, H. R. Krishnamurthy, A. K. Geim, A. C. Ferrari, A. K. Sood, *Nat. Nanotechnol.* **2008**, *3*, 210.
[179] Y. Jin, D. H. Keum, S.-J. An, J. Kim, H. S. Lee, Y. H. Lee, *Adv. Mater.* **2015**, *27*, 5534.
[180] A. Pospischil, M. M. Furchi, T. Mueller, *Nat. Nanotechnol.* **2014**, *9*, 257.
[181] Y. Katagiri, T. Nakamura, A. Ishii, C. Ohata, M. Hasegawa, S. Katsumoto, T. Cusati, A. Fortunelli, G. Iannaccone, G. Fiori, S. Roche, J. Haruyama, *Nano Lett.* **2016**, *16*, 3788.
[182] H. Huang, W. Xu, T. Chen, R.-J. Chang, Y. Sheng, Q. Zhang, L. Hou, J. H. Warner, *ACS Appl. Mater. Interfaces* **2018**, *10*, 37258.
[183] E. Margapoti, J. Li, Ö. Ceylan, M. Seifert, F. Nisic, T. L. Anh, F. Meggendorfer, C. Dragonetti, C.-A. Palma, J. V. Barth, J. J. Finley, *Adv. Mater.* **2015**, *27*, 1426.
[184] J. M. Mativetsky, G. Pace, M. Elbing, M. A. Rampi, M. Mayor, P. Samorì, *J. Am. Chem. Soc.* **2008**, *130*, 9192.
[185] V. Ferri, M. Elbing, G. Pace, M. D. Dickey, M. Zharnikov, P. Samorì, M. Mayor, M. A. Rampi, *Angew. Chem., Int. Ed.* **2008**, *47*, 3407.

[186] K. S. Novoselov, A. Mishchenko, A. Carvalho, A. H. Castro Neto, *Science* **2016**, *353*, aac9439.
[187] B. W. H. Baugher, H. O. H. Churchill, Y. Yang, P. Jarillo-Herrero, *Nat. Nanotechnol.* **2014**, *9*, 262.
[188] D. Li, M. Chen, Z. Sun, P. Yu, Z. Liu, P. M. Ajayan, Z. Zhang, *Nat. Nanotechnol.* **2017**, *12*, 901.
[189] H.-M. Li, D. Lee, D. Qu, X. Liu, J. Ryu, A. Seabaugh, W. J. Yoo, *Nat. Commun.* **2015**, *6*, 6564.
[190] M. S. Choi, D. Qu, D. Lee, X. Liu, K. Watanabe, T. Taniguchi, W. J. Yoo, *ACS Nano* **2014**, *8*, 9332.
[191] G. Wang, L. Bao, T. Pei, R. Ma, Y.-Y. Zhang, L. Sun, G. Zhang, H. Yang, J. Li, C. Gu, S. Du, S. T. Pantelides, R. D. Schrimpf, H.-J. Gao, *Nano Lett.* **2016**, *16*, 6870.
[192] S. Vélez, D. Ciudad, J. Island, M. Buscema, O. Txoperena, S. Parui, G. A. Steele, F. Casanova, H. S. J. van der Zant, A. Castellanos-Gomez, L. E. Hueso, *Nanoscale* **2015**, *7*, 15442.
[193] C. Jia, A. Migliore, N. Xin, S. Huang, J. Wang, Q. Yang, S. Wang, H. Chen, D. Wang, B. Feng, Z. Liu, G. Zhang, D.-H. Qu, H. Tian, M. A. Ratner, H. Q. Xu, A. Nitzan, X. Guo, *Science* **2016**, *352*, 1443.
[194] H. B. Akkerman, P. W. M. Blom, D. M. de Leeuw, B. de Boer, *Nature* **2006**, *441*, 69.
[195] C. Jia, B. Ma, N. Xin, X. Guo, *Acc. Chem. Res.* **2015**, *48*, 2565.
[196] T. Leydecker, M. Herder, E. Pavlica, G. Bratina, S. Hecht, E. Orgiu, P. Samorì, *Nat. Nanotechnol.* **2016**, *11*, 769.
[197] S. L. Broman, S. Lara-Avila, C. L. Thisted, A. D. Bond, S. Kubatkin, A. Danilov, M. B. Nielsen, *Adv. Funct. Mater.* **2012**, *22*, 4249.
[198] D. Kim, H. Jeong, H. Lee, W.-T. Hwang, J. Wolf, E. Scheer, T. Huhn, H. Jeong, T. Lee, *Adv. Mater.* **2014**, *26*, 3968.
[199] S. Seo, M. Min, S. M. Lee, H. Lee, *Nat. Commun.* **2013**, *4*, 1920.
[200] E. Margapoti, P. Strobel, M. M. Asmar, M. Seifert, J. Li, M. Sachsenhauser, Ö. Ceylan, C.-A. Palma, J. V. Barth, J. A. Garrido, A. Cattani-Scholz, S. E. Ulloa, J. J. Finley, *Nano Lett.* **2014**, *14*, 6823.
[201] M. Döbbelin, A. Ciesielski, S. Haar, S. Osella, M. Bruna, A. Minoia, L. Grisanti, T. Mosciatti, F. Richard, E. A. Prasetyanto, L. De Cola, V. Palermo, R. Mazzaro, V. Morandi, R. Lazzaroni, A. C. Ferrari, D. Beljonne, P. Samorì, *Nat. Commun.* **2016**, *7*, 11090.
[202] Y. Shao, M. F. El-Kady, L. J. Wang, Q. Zhang, Y. Li, H. Wang, M. F. Mousavi, R. B. Kaner, *Chem. Soc. Rev.* **2015**, *44*, 3639.
[203] X. Yang, C. Cheng, Y. Wang, L. Qiu, D. Li, *Science* **2013**, *341*, 534.
[204] Z. Lei, N. Christov, X. S. Zhao, *Energy Environ. Sci.* **2011**, *4*, 1866.
[205] J. L. Vickery, A. J. Patil, S. Mann, *Adv. Mater.* **2009**, *21*, 2180.
[206] C. Liu, Z. Yu, D. Neff, A. Zhamu, B. Z. Jang, *Nano Lett.* **2010**, *10*, 4863.
[207] G. Wang, X. Sun, F. Lu, H. Sun, M. Yu, W. Jiang, C. Liu, J. Lian, *Small* **2012**, *8*, 452.
[208] Y. Si, E. T. Samulski, *Chem. Mater.* **2008**, *20*, 6792.
[209] L. Hu, F. La Mantia, H. Wu, X. Xie, J. McDonough, M. Pasta, Y. Cui, *Adv. Energy Mater.* **2011**, *1*, 1012.
[210] J. Xia, F. Chen, J. Li, N. Tao, *Nat. Nanotechnol.* **2009**, *4*, 505.
[211] Q. Ke, J. Wang, *J. Materiomics* **2016**, *2*, 37.
[212] E. Orgiu, J. George, J. A. Hutchison, E. Devaux, J. F. Dayen, B. Doudin, F. Stellacci, C. Genet, J. Schachenmayer, C. Genes, G. Pupillo, P. Samorì, T. W. Ebbesen, *Nat. Mater.* **2015**, *14*, 1123.